THE GEOLOGICAL SOCIETY OF AMERICA®

Stratigraphic record of the asteroidal Veritas breakup in the Tortonian Monte dei Corvi section (Ancona, Italy)

Alessandro Montanari[1,†], Ken Farley[2,†], Philippe Claeys[3,†], David De Vleeschouwer[4,†], Niels de Winter[3,†], Stef Vansteenberge[3,†], Matthias Sinnesael[3,†], and Christian Koeberl[5,6,†]

[1]*Osservatorio Geologico di Coldigioco, Contrada Coldigioco 4, 62021 Apiro, Italy*
[2]*Caltech Division of Geological and Planetary Sciences, MS 170-25, Pasadena, California 91125, USA*
[3]*Department of Earth System Science DGLG-WE, Vrije Universiteit Brussel, Pleinlaan 2, B-1050 Brussels, Belgium*
[4]*Center for Marine Environmental Science (MARUM), Leobener Strasse, 28359 Bremen, Germany*
[5]*Department of Lithospheric Research, Center for Earth Sciences, University of Vienna, Althanstrasse 14, A-1090 Vienna, Austria*
[6]*Natural History Museum, Burgring 7, A-1010 Vienna, Austria*

ABSTRACT

The discovery of elevated concentrations of the cosmogenic radionuclide ^{3}He in deep-sea sediments from Ocean Drilling Program (ODP) Site 926 (Atlantic Ocean) and ODP Site 757 (Indian Ocean) points toward accretion of extraterrestrial matter, probably as a result of the catastrophic disruption of a large asteroid that produced the Veritas family of asteroids at ca. 8.3 ± 0.5 Ma, and which may have had important effects on the global climatic and ecologic systems. Here, we investigated the signatures possibly related to the Veritas event by performing a high-resolution multiproxy stratigraphic analysis through the late Tortonian–early Messinian Monte dei Corvi section near Ancona, Italy. Closely spaced bulk-rock samples through a 36-m-thick section, approximately spanning from ca. 9.9 Ma to ca. 6.4 Ma, show an ~5-fold ^{3}He anomaly starting at ca. 8.5 Ma and returning to background values at ca. 6.9 Ma, confirming the global nature of the event. We then analyzed, at 5 cm intervals, bulk-rock samples for sedimentary and environmental proxies such as magnetic susceptibility, calcium carbonate content, total organic carbon, and bulk carbonate δ^{18}O and δ^{13}C, through a 21-m-thick section encompassing the ^{3}He anomaly. Available high-resolution sea-surface temperature data (via alkenone analyses) for this site show a temperature decrease starting exactly at the inception of the ^{3}He anomaly. Cyclostratigraphic fast-Fourier-transform spectral analyses of the proxies indicate an age of 8.47 ± 0.05 Ma for the inception of the ^{3}He anomaly. A search for impact ejecta (analogous to what is present in the late Eocene, where both a ^{3}He anomaly and large-scale impact events are recorded) was not successful. Detailed cyclostratigraphic analyses of our data suggest that the changes in the stable isotope series and environmental proxy series through this late Tortonian time interval had a common forcing agent, and that perturbations of orbitally forced climate cycles are present exactly through the interval with the enhanced influx of extraterrestrial ^{3}He. Thus, the chemostratigraphic evidence for a collisional event that created the Veritas family of asteroids, coinciding with climate perturbations on Earth, suggests yet another form of interaction between Earth and the solar system.

INTRODUCTION

Geologic Setting

As a consequence of the Cretaceous-to-present tectono-sedimentary evolution of the Northern Apennines accretionary wedge, as synthetically illustrated in Figure 1A (e.g., D'Argenio, 1970; Alvarez et al., 1974; Channell et al., 1979; Castellarin et al., 1982; Treves, 1984; Marroni et al., 2001; Cornamusini et al., 2002; Argnani et al., 2006, and references therein), the complete and continuous Jurassic to early Miocene pelagic succession of the Umbria-Marche Basin, for example, in the type locality of Gubbio, is interrupted in the mid-Miocene by the arrival of the siliciclastic turbidites of the Marnoso-Arenacea Flysch. The much-celebrated stratigraphic completeness of the classic Gubbio pelagic succession has, in the past half a century or so, contributed considerably to the ever-improving resolution of event and integrated stratigraphy of Earth history (e.g., Menichetti et al., 2016, and references therein). However, with the arrival of the flysch, detailed integrated stratigraphic study cannot be extended into the Miocene. This interruption did not occur in the easternmost part of the Umbria-Marche Basin, along the Cònero Riviera, which extends along the anticlinal Adriatic promontory between the city of Ancona and Monte Cònero (for location, see Fig. 1A). Here, turbidite-free, pelagic and hemipelagic carbonates covering the entire Miocene Epoch all the way up to the early Pliocene are continuously exposed on sea cliffs. In particular, the monoclinal sections covering the Langhian to early Pliocene portion of this pelagic succession on the eastern cliffs of Monte dei Corvi (for location, see Fig. 1B) have, in recent years, promoted high-resolution integrated stratigraphic studies of mid- and late Miocene events, including biostratigraphic, chemostratigraphic, magnetostratigraphic events and their radioisotopic and astrochronologic calibrations (Montanari et al., 1997; Cleaveland et al., 2002; Hilgen et al., 2003; Mader et al., 2004; Hüsing et al., 2010; Wotzlaw et al., 2014; Tzanova et al., 2015). The global stratotype section and point (GSSP) for the base of the Tortonian Stage was established in the Monte dei Corvi section by Hilgen et al. (2005). Recently, the stratigraphic stretch comprising the Upper Tortonian to the basal Messinian exposed in a new Monte dei Corvi Beach section, i.e., the stratigraphical equivalent of the La Sardella section of Montanari et al. (1997) exposed up high on the Monte dei Corvi cliff (Fig. 1B), was proposed by Hüsing et al. (2007)

†sandro.coldigioco@gmail.com, farley@gps.caltech.edu, phclaeys@vub.ac.be, ddevleeschouwer@marum.de, nidewint@vub.ac.be, svsteenb@vub.ac.be, matthias.sinnesael@vub.ac.be, christian.koeberl@univie.ac.at.

GSA Bulletin; September/October 2017; v. 129; no. 9/10; p. 1357–1376; doi: 10.1130/B31476.1; 13 figures; Data Repository item 2017149; published online 23 June 2017.

For permission to copy, contact editing@geosociety.org
© 2017 Geological Society of America

Downloaded from https://pubs.geoscienceworld.org/gsa/gsabulletin/article-pdf/129/9-10/1357/2615686/1357.pdf
by University of Western Ontario user

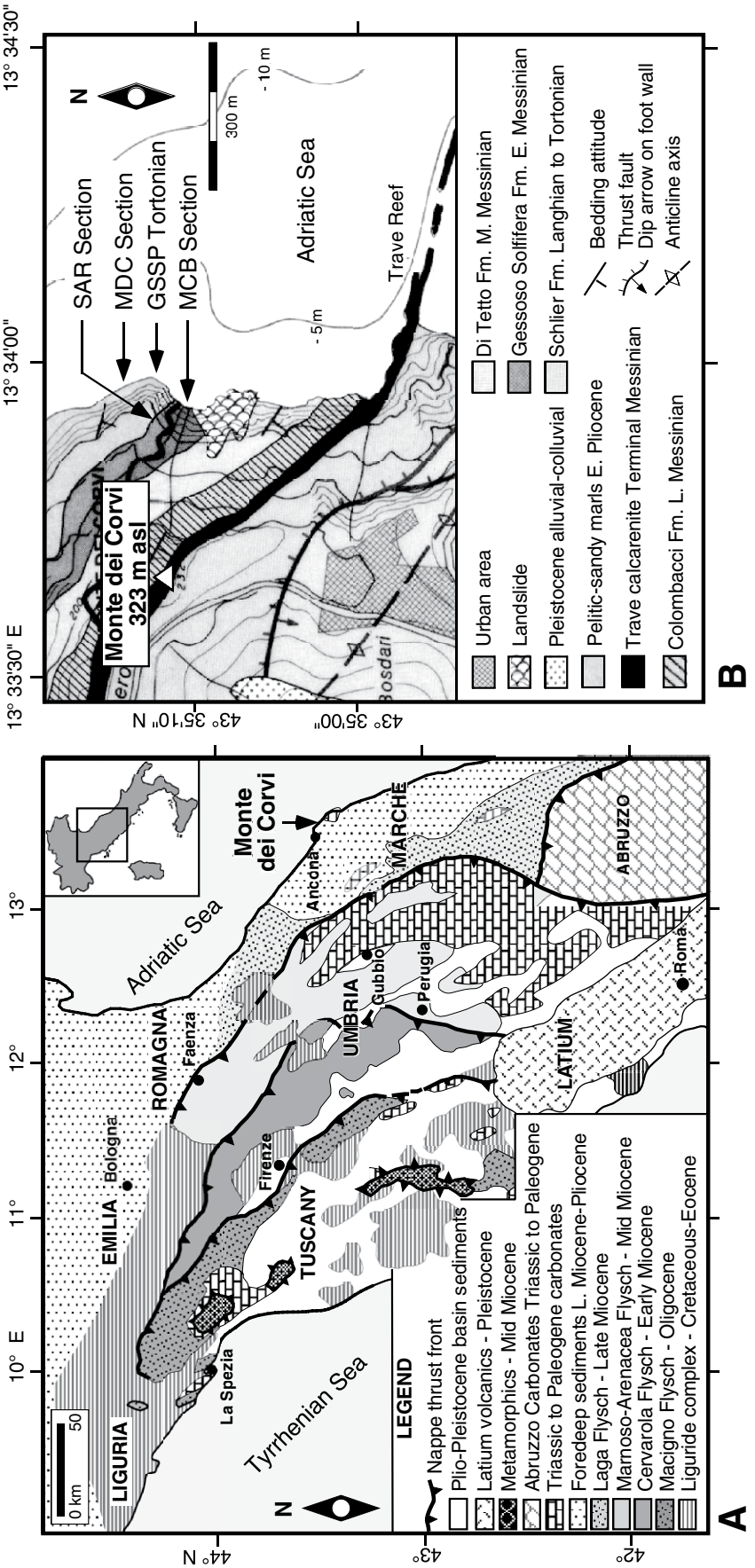

Figure 1. (A) Simplified geologic-structural map of the Northern Apennines accretionary wedge, and location of the Monte dei Corvi section. (B) Geologic map of the Monte dei Corvi area (after Coccioni et al., 1993) with the location of the Sardella (SAR), Monte dei Corvi (MDC), and Monte dei Corvi Beach (MCB) sections, and the global stratotype section and point (GSSP) for the Serravallian-Tortonian Stage boundary.

Downloaded from https://pubs.geoscienceworld.org/gsa/gsabulletin/article-pdf/129/9-10/1357/2615686/1357.pdf
by University of Western Ontario user

as a complete Mediterranean reference section for the Tortonian Stage.

Late Tortonian Extraterrestrial Event

In addition to the constriction of the Mediterranean-Atlantic connection and consequent inception of the Messinian salinity crisis (Hsü et al., 1973, 1978; Krijgsman et al., 1999), the late Tortonian hosted another exceptional event, which may have had important effects on global climatic and ecologic systems—an extraterrestrial event consisting of the catastrophic disruption of a 140 km diameter asteroid, probably due to a collision in the asteroid belt, which produced the Veritas family of asteroids ca. 8.3 ± 0.5 Ma (Nesvorny et al., 2003). Further astrophysical studies by Knežević et al. (2006) indicated that the Veritas family may actually be made up by several groups of asteroids, the origin of which may be traced back to ca. 8.9 Ma, an age similar to, but slightly older than, the one computed by Nesvorny et al. (2003). The concept that the Veritas family actually comprises multiple asteroid groups was also advocated by Michel et al. (2010). In any case, the discovery by Nesvorny and coworkers predicted that, as a consequence of the Veritas breakup, Earth would have been subjected to an enhanced flux of interplanetary dust particles, which, in their journey from the asteroid belt to Earth, would have been enriched in the cosmogenic radionuclide ^{3}He. Following the study of Nesvorny et al. (2003), Farley et al. (2006) discovered a fivefold increase in ^{3}He concentration in late Tortonian deep-sea sediments from Ocean Drilling Program (ODP) Site 926 (Atlantic Ocean) and ODP Site 757 (Indian Ocean), seemingly fulfilling the prediction of Nesworny and coworkers. Unfortunately, ODP core Site 757 has a poor chronostratigraphic definition (due to a very low sedimentation rate), whereas the ODP Site 926 record does not extend sufficiently up section to establish precisely when the anomalous ^{3}He flux returns to a background value. Nevertheless, the extremely rapid increase of the ^{3}He concentration in these late Tortonian sediments appears to confirm the global nature of this extraterrestrial event.

METHODS AND TECHNIQUES

To search for signatures possibly related to the Veritas event, we performed a high-resolution multiproxy stratigraphic analysis through the Upper Tortonian–Lower Messinian Monte dei Corvi Beach section. For this, we followed the sedimentological and stratigraphic descriptions and bed numbering of Hüsing et al. (2009), as shown in Figure 2A. First, we collected closely spaced bulk-rock samples for ^{3}He analysis through a 36-m-thick section spanning from 106 m to 142 m, and we found the ~5-fold ^{3}He anomaly starting at ~120 m and returning to background values at ~136 m (Fig. 2B). We then analyzed, at 5 cm intervals, bulk-rock samples for sedimentary and environmental proxies such as magnetic susceptibility, calcium carbonate content, total organic carbon via loss on ignition (LOI) analysis, δ^{18}O, and δ^{13}C, through a 21-m-thick section encompassing the ^{3}He anomaly. Alkenone analyses on closely spaced samples were obtained to derive a high-resolution sea-surface temperature (SST) profile (Fig. 2C) for this Mediterranean site from the same Monte dei Corvi Beach section by Tzanova et al. (2015). Finally, we used the five high-resolution proxy series plotted in Figures 3C–3D to perform cyclostratigraphic spectral analysis. The magnetic susceptibility (MS) series, which yielded the most stationary frequency power spectra (see later herein), led to the identification of long and short eccentricity cycles, and the tuning of the Monte dei Corvi Beach section using the solution of Laskar et al. (2004), which indicated an age of 8.5 Ma for the inception of the ^{3}He anomaly (Fig. 2D).

Helium isotope analyses were performed at the California Institute of Technology (Pasadena, California) following the method of Mukhopadhyay et al. (2001). The analytical results are shown in Table DR1 in the GSA Data Repository.[1]

MS analyses were performed on ~40 g, <5-mm-grain-size dry-crushed (in brass mortar and pestle) bulk samples at Osservatorio Geologico di Coldigioco (OGC, Apiro, Italy) using a Bartington MS2B dual-frequency magnetometer at low frequency (0.465 kHz) and ×0.1 sensitivity, averaging three measurements for each sample, and values were mass corrected. Results are shown in Table DR2 in the GSA Data Repository (see footnote 1).

Calcium carbonate content (wt% $CaCO_3$) in 420 bulk-rock samples through the 110–131 m interval was measured at the OGC with a Dietrich-Frühling water calcimeter (±2.5% precision). Calibration was done using a Carrara marble standard. Results are shown in Table DR2 in the GSA Data Repository (see footnote 1). Total organic carbon in weight percent was obtained at OGC by LOI of dried (at 110 °C in an oven) and powdered ~5 g bulk samples in a large Tornati Forni electric kiln with programmable pyrometer (400 samples at a time in aluminum caps), at 360 °C for 6 h. The LOI was obtained by weight difference measured with a 1-mg-precision electronic scale. Results are shown in Table DR2 in the GSA Data Repository (see footnote 1).

Stable isotope measurements for δ^{13}C (in per mil [‰] relative to Vienna Peedee belemnite [V-PDB]) and δ^{18}O (‰, V-PDB) were carried out on bulk-rock samples at the Vrije Universiteit Brussel using both a dual-inlet ThermoFinnigan delta+XL isotope ratio mass spectrometer (IRMS) interfaced with an automated Kiel III device for carbonates, and a Nu Perspective IRMS interfaced with a Nu Carb automated carbonate device for highly sensitive, ultra-precise isotopic measurements in an automated, high-throughput workflow. Acidification of the samples occurred at a temperature of 70 °C for both instruments. Corrections were carried out using the in-house standard MAR-2, which is made of Marbella limestone and has been calibrated against the international standard NBS-19. On the basis of replicated measurements on standards and sampled material, the reproducibility for both mass spectrometers on the carbon and oxygen isotopes was estimated at 0.05‰ (1σ) and 0.15‰ (1σ), respectively. Results are shown in Table DR2 in the GSA Data Repository (see footnote 1).

The parts per million (ppm) and parts per billion (ppb) contents of 41 trace elements from a selected collection of 23 samples from meter level 13.5 up to meter level 131.0 were analyzed by X-ray fluorescence (XRF) and instrumental neutron activation analysis (INAA) at the University of Vienna following the methods described by Mader and Koeberl (2009) for INAA and Huber et al. (2014) for XRF. Results are shown in Table DR3 in the GSA Data Repository (see footnote 1).

We conducted spectral analyses of the 5-cm-resolution proxy series spanning from 110 to 131 m level ($CaCO_3$, MS, LOI, C_{org}, δ^{18}O, and δ^{13}C) in MATLAB using algorithms of Bice et al. (2011), modified from Muller and MacDonald (2000). In short, we produced periodograms by performing fast Fourier transforms (FFTs) of the data (detrended and padded with zeros) in the stratigraphic domain, which yielded a set of spectral peaks representing the stratigraphic wavelengths (periods) of the cycles. We evaluated the statistical significance of spectral peaks by generating a 95% confidence level (C.L.) from a Monte Carlo noise simulation (Muller and MacDonald, 2000). The persistence of the spectral peaks through the stratigraphic section was evaluated through the use of an evolutionary, or sliding window, FFT. The window size was chosen to be about one third of the whole stratigraphic interval analyzed, which is large

[1]GSA Data Repository item 2017149, Tables DR1–DR4, is available at http://www.geosociety.org/datarepository/2017 or by request to editing@geosociety.org.

Downloaded from https://pubs.geoscienceworld.org/gsa/gsabulletin/article-pdf/129/9-10/1357/2615686/1357.pdf
by University of Western Ontario user

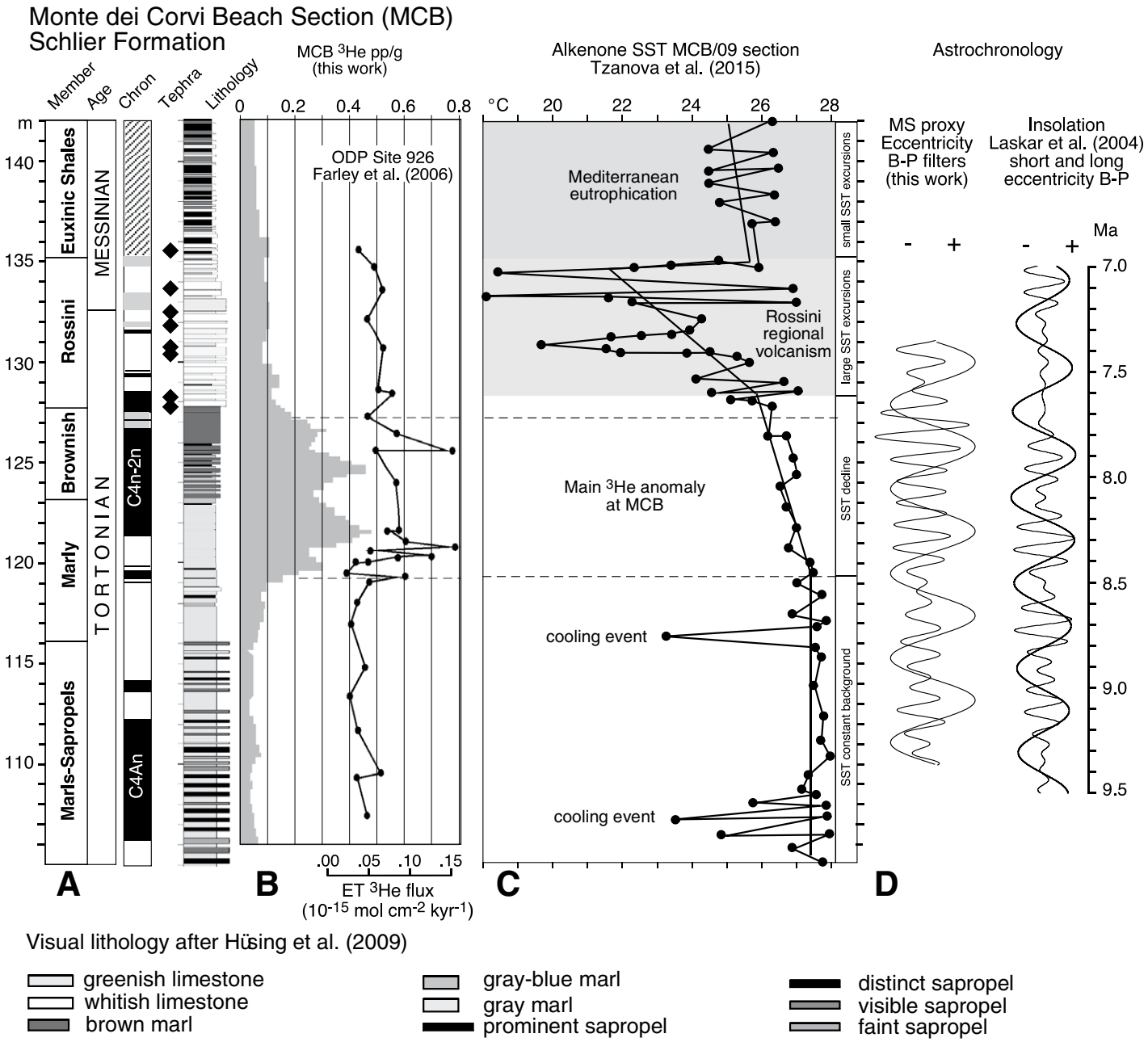

Figure 2. Synoptic stratigraphic scheme of the Monte dei Corvi Beach section. (A) Chronostratigraphy, magnetostratigraphy, and lithostratigraphy after Hüsing et al., (2007, 2009). (B) ^{3}He stratigraphy (this work; in 10–12 cm^3 per gram of bulk sample [pp/g]) compared to Ocean Drilling Program (ODP) Site 926 of Farley et al. (2006). ET—extraterrestrial. (C) Sea-surface temperature (SST) profile after Tzanova et al. (2015), highlighting major environmental events recorded in the Monte dei Corvi Beach section. (D) Astronomical time scale and tuning of the Monte dei Corvi Beach magnetic susceptibility (MS) series (this work) to the Laskar et al. (2004) eccentricity curve by means of band-pass (B-P) curves.

enough to enable the detection of short and long eccentricity signals given the mean sedimentation rate of the studied interval. Astronomical tuning and ultimate dating of local and global environmental and climatic events, as well as the inception of the ^{3}He anomaly recorded in Monte dei Corvi Beach section, was accomplished through the use of broad band-pass filtering of the MS proxy series, which appears to be the most consistent and least-disturbed proxy series recording Milankovitch cycles. Variations in the MS proxy series between 300 and 500 k.y. were isolated for the long eccentricity cycle (405 k.y. period). These filtered data were then used for correlation via constrained pattern matching with the theoretical eccentricity curve of Laskar et al. (2004). We performed the actual tuning of the composite section by correlating the maxima of a broad 300–500 k.y. band-pass curve of the MS time series with the maxima of the band-pass eccentricity curve of Laskar et

Downloaded from https://pubs.geoscienceworld.org/gsa/gsabulletin/article-pdf/129/9-10/1357/2615686/1357.pdf
by University of Western Ontario user

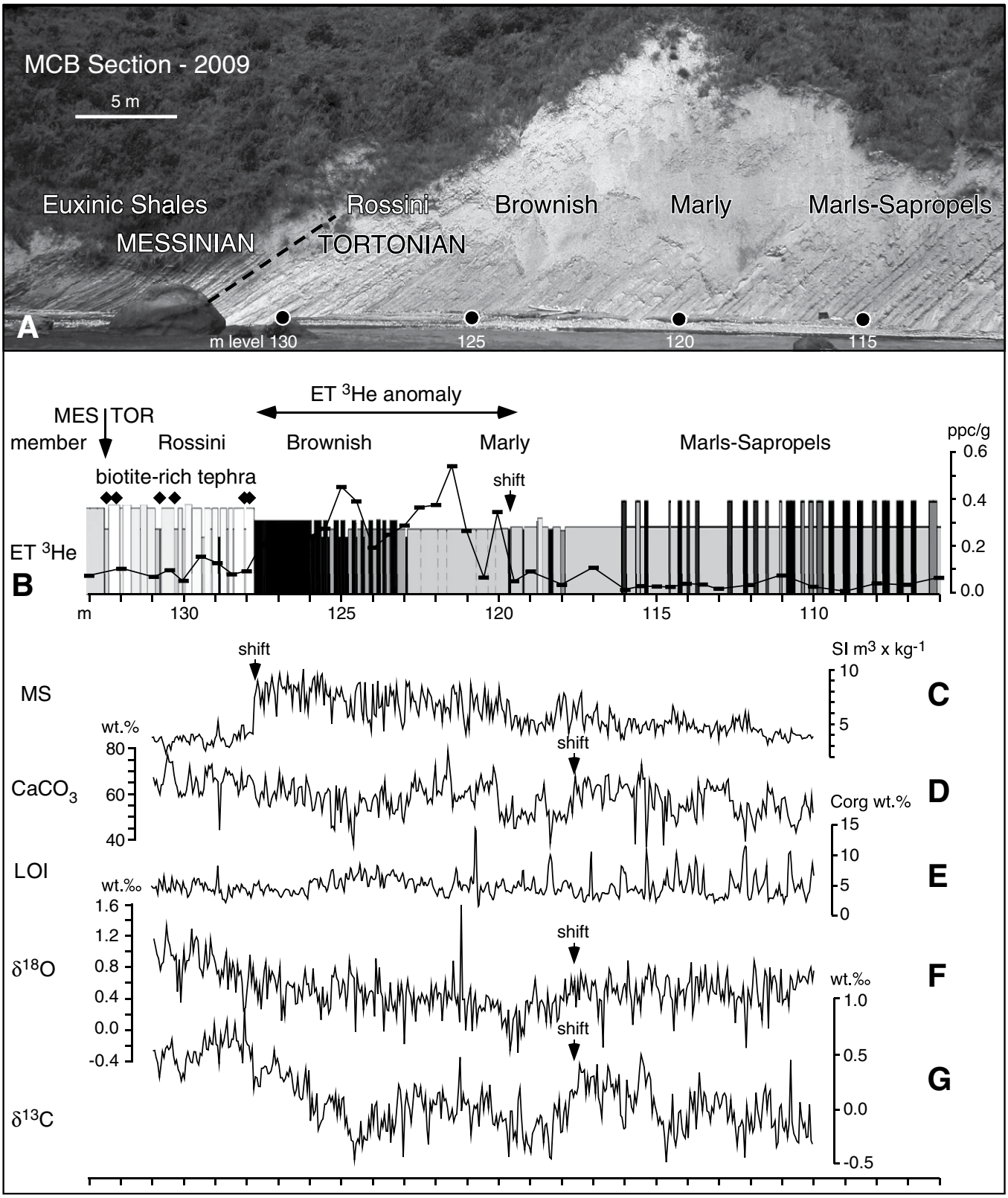

Figure 3. (A) Panoramic view of the upper Monte dei Corvi Beach section as it was excellently exposed in 2009, showing the location of the Tortonian-Messinian boundary, and the succession of lithostratigraphic members described in the text. The sample-to-sample series of ^{3}He abundance is plotted over the detailed lithologic log of Hüsing et al. (2009). (B) Extraterrestrial (ET) ^{3}He (in 10–12 cm^3 per gram of bulk sample [ppc/g]). (C) Magnetic susceptibility (MS), (D) $CaCO_3$ (wt%), (E) loss on ignition (LOI) C_{org} (wt%), (F) $\delta^{18}O$ (‰), and (G) $\delta^{13}C$ (‰) series are plotted according to the same lithologic log of Hüsing et al. (2009). MES—Messinian; TOR—Toronian.

Downloaded from https://pubs.geoscienceworld.org/gsa/gsabulletin/article-pdf/129/9-10/1357/2615686/1357.pdf
by University of Western Ontario user

al. (2004). The rationale for matching maxima in MS with maxima in eccentricity is based on the fact that marly sediments contain a higher component of magnetic terrigenous material than limestones, thus reflecting warm and wet climate conditions in a glacio-eustatic climate system such as the one of the midlatitude western Tethys, and these warm and wet conditions occur during eccentricity maxima (e.g., Cleaveland et al., 2002).

LITHOLOGICAL, CHEMICAL, AND MAGNETIC DATA: RESULTS

Lithostratigraphic and Sedimentologic Analysis

The Monte dei Corvi Beach section was well exposed (cleaned and completely uncovered) along the straight and flat-surfaced littoral bluff at the foot of Monte dei Corvi until the summer of 2009, allowing Hüsing et al. (2007, 2009) to carry out an extremely detailed lithologic log, which greatly facilitated our effort to obtain accurate, closely spaced sampling (Fig. 3A). The overall Monte dei Corvi Beach section is devoid of soft sediment slumping or tectonic deformations, such as faulting, kink folding, pressure-solution cleavage, or pseudobedding stylolitization (sensu Alvarez et al., 1985). In a few places, fibrous-calcite slickenside surfaces parallel to bedding (or at a very low angle to it) indicate mild shearing due to flexural slip folding (see fig. 2 *in* Hüsing et al., 2009). Because of the ideal exposure conditions in the late 2000s, it was possible to subdivide what was originally termed the Tortonian Marly Member of the Schlier Formation by Montanari et al. (1997) into a succession of lithostratigraphic members based on the detailed lithologic logs of Hilgen et al. (2005), and Hüsing et al. (2007, 2009). Taking as reference level the GSSP for the Tortonian in the upper part of the Calcareous Member of the Schlier Formation at meter level 63.2 (Hilgen et al., 2005), the base of the Marls-Sapropels Member can be placed at meter level 83.0, where dark, recessive sapropelic horizons start to rhythmically alternate with gray, prominent marl and marly limestone layers (Fig. 3A). These lithologies represent midbathyal pelagic sediments, the carbonate component of which is mostly made up of high-Mg biogenic calcite from planktonic foraminifera and coccoliths, with minor benthic calcareous foraminifera and rare ostracods, whereas the siliciclastic component is made up of hemipelagic, terrigenous silt and clay of probable eluvial origin; i.e., it originated from the erosion and runoff of the emerging Alpine orogen. Marls and marly limestone layers are strongly bioturbated, showing conspicuous fossil traces of *Planolites*, which suggest a fairly well-oxygenated and nutrient-rich paleoseafloor. Good preservation of planktonic foraminiferal tests and calcareous nannofossils in these carbonate sediments, including sapropelic marls, through the Tortonian and early Messinian portion of the Monte dei Corvi succession (Montanari et al., 1997) suggests high pH conditions in the depositional and diagenetic environments.

At meter level 116, the last visible sapropelic marl marks the top of the Marls-Sapropels Member, which is overlain by a 7-m-thick plain Marly Member (Fig. 3A). In this interval, Hüsing et al. (2009) reported only four thin sapropelic horizons between 117.9 and 119.7 m. From meter level 119.7 to 122.9, the Marly Member loses evident bedding and is completely devoid of visible sapropelic horizons.

Clear bedding, as defined by alternating, more or less recessive marls, reappears above meter level 122.9, where these sediments assume a light-brown tinge, which Hüsing et al. (2009) referred to as the "brownish interval" up to meter level 127.8. The lower part of this Brownish Member actually consists of an alternation of gray-blue and brown marly layers, whereas the upper part is made up of practically homogeneous or very faintly bedded brown marls (see fig. 3b *in* Hüsing et al., 2009).

Above the Brownish Member, an ~7.5-m-thick package of well-bedded, hard, whitish marly limestones, called the Rossini Member by Montanari et al. (1997), contains eight volcanosedimentary layers (Hüsing et al., 2009; Wotzlaw et al., 2014), some of which have abundant biotite. An equivalent unit is also present in Upper Tortonian–Lower Messinian sections in the Romagna Apennines near Faenza, some 160 km NW from Monte dei Corvi (Vai, 1997; Odin et al., 1997a; Laurenzi et al., 1997; for location, see Fig. 1A). Although the provenance of the Rossini tephra is not yet known, it provides evidence of rather intense explosive volcanism in the vicinity of the Umbria-Marche Basin. The Tortonian-Messinian chronostratigraphic boundary was traced by Hüsing et al. (2009) along the sixth volcanosedimentary layer at meter level 132.5, and approximated to the first regular occurrence of planktonic foraminifer *Globorotalia miotumida* (*Globorotalia conomiozea* group). At about the same stratigraphic level in the Sardella section, Montanari et al. (1997) placed the Tortonian-Messinian boundary at the first occurrence of *G. conomiozea.* Vai (1997), Odin et al. (1997a), and Laurenzi et al. (1997) did the same in their Faenza sections.

At about meter level 135.3, some 40 cm below the eighth volcanosedimentary layer, the first black shale layer, actually a planktonic foraminiferal marl with a relatively high concentration of organic carbon (kerogen), marks the base of the Euxinic Shales unit. This unit consists of a rhythmic alternation of more or less biogenic carbonate-rich sapropelic marls, giving it the visual appearance of a striped black-and-white succession.

Extraterrestrial Signatures

The extraterrestrial ^{3}He profile in Figure 3B shows a fairly regular background abundance around a mean of $0.06 \pm 0.04\ 10^{-12}$ cm^3 per gram of bulk sample (pcm^3/g) up to meter level 119.5 and then a sharp increase in the next sample at 120.0 m up to 0.35 pcm^3/g. It is in between these two samples, thus at 119.75 ± 0.25 m in the Monte dei Corvi Beach section, where we place the inception of the high influx of interplanetary dust particles. After a return to background level in sample 120.5 m, ^{3}He concentration shoots up again, reaching a peak of 0.55 pcm^3/g, at 121.5 m and then gradually descend to a low of 0.2 pcm^3/g at 124.0 m, which is still higher than the mean background value of ~0.06 pcm^3/g. This low is followed by yet another sharp increase reaching a third peak of 0.45 pcm^3/g at 125.0 m and then return to a value of 0.1 pcm^3/g at meter level 128.0, which is close to but not quite at background level. At 129.5 m, the ^{3}He concentration rises up again to a small peak of 1.5 pcm^3/g and then descends again at 130.0 m to a mean of 0.1 pcm^3/g all through the Rossini Member (see Fig. 2B). At 135 m, coinciding with the base of the Euxinic Shales Member, the mean ^{3}He concentration returns definitively to the initial background level of ~0.06 pcm^3/g. In summary, the inception of the extraterrestrial ^{3}He anomaly can be confidentially placed at 119.75 ± 0.25 m in the Monte dei Corvi Beach section, whereas the end of it is tentatively placed at ~135.0 m.

After confirming the anomalously high ^{3}He concentration through the Monte dei Corvi Beach section, which indicates a higher-than-normal flux of extraterrestrial matter to Earth, we attempted to detect the proverbial (extraterrestrial) needle in the (sedimentary) haystack (e.g., Montanari et al., 1998; Montanari and Koeberl, 2000) by analyzing a suite of 23 samples for trace-element contents. The aim was to detect a possible chondritic signature, i.e., elevated concentrations of platinum group elements (PGEs) such as iridium, and other siderophile elements, including nickel and cobalt, but also chromium and gold. These trace elements are significantly more abundant in meteorites than they are in terrestrial crustal rocks and are thus often used as proxies for a meteoritic component (see review by Koeberl, 2014). Iridium and gold

Downloaded from https://pubs.geoscienceworld.org/gsa/gsabulletin/article-pdf/129/9-10/1357/2615686/1357.pdf
by University of Western Ontario user

concentrations turned out to be below the detection limit in all the analyzed samples (Table DR3 in the GSA Data Repository [see footnote 1]), whereas Ni, Co, and Cr concentrations mimic fairly well the concentration of the terrigenous component (i.e., 100 – [$CaCO_3$ + LOI] wt%) in each sample, and that of Sc in fact serves as a good tracer for terrestrial composition (Fig. 4A). On the other hand, when Ni, Cr, and Co are normalized to the terrigenous component, i.e., Ni/Sc, Cr/Sc, and Co/Sc, their excess abundance is emphasized (Fig. 4B). In particular, the sample at 120.0 m, which corresponds to the first peak of extraterrestrial ^{3}He, shows a clear excess in Ni, although no apparent excess in Co or in Cr seems to be present. On the other hand, the Ni/Sc, Cr/Sc, and Co/Sc ratios all peak in samples 121.5 m and 122.0 m, where ^{3}He shows the second and largest peak in the main extraterrestrial He anomaly interval. We note that Ni/Sc and Co/Sc, and to a minor extent Cr/Sc, show distinct peaks at 128.05 m and 129.5 m in samples from the first two volcanic ashes of the Rossini Member, while ^{3}He/Sc is at a relative low in these samples. All this suggests that the Ni excess at 120.0 m and 122.0 m may be due to addition of meteoritic material, perhaps Ni-rich spinel, which is often used as a tracer of cosmic events in the sedimentary record (e.g., Ferriére and Robin, 2009, and references therein). On the other hand, the excess concentrations of Ni and Co in the two volcanic ashes are more likely due to Ni- and Co-rich mineral phases contained in the fallout tephra. In any case, we did not find the extraterrestrial PGE needle in the Monte dei Corvi Beach section, which suggests to us that the cascade of interplanetary dust particles during the presumed Veritas breakup event, as represented by the ^{3}He anomaly, was not accompanied by large meteoritic impacts, such as the ones recorded in the late Eocene in the GSSP section of Massignano (Montanari et al., 1993; Farley et al., 1998), nor extensive micrometeorite showers. Eventually, a search for trace amounts of PGEs on more closely spaced samples may reveal the presence of impactoclastic layers or the influx of meteorites during the Veritas interplanetary dust particle cascade.

Magnetic Susceptibility

The MS profile of the Monte dei Corvi Beach section (Fig. 3D) shows an overall monotonic increase from ~4 SI m^3 kg^{-1} to ~8 SI m^3 kg^{-1} up to meter level 127.8 (the base of the Rossini Member). At exactly 127.8 m, the MS sharply shifts down to initial values of ~4 SI m^3 kg^{-1} all through the lower part of the Rossini Member. Through the Marls-Sapropels Member up to 116 m, the MS profile is characterized by relatively low-amplitude excursions of about ±1.5 SI m^3 kg^{-1}, whereas through the Marly Member up to meter level 127.8, MS excursions show higher amplitudes of about ±2.5 SI m^3 kg^{-1}. However, in the short interval between 118.3 and 119.7 m, the MS signal has mean values of ~5 SI m^3 kg^{-1}, with relatively low-amplitude excursions of about ±1 SI m^3 kg^{-1}. Our high-resolution MS profile is remarkably similar to the more sparsely sampled MS profile of Hüsing et al. (2009) through the same Monte dei Corvi Beach section (Fig. 5), suggesting that MS measurements were accurate.

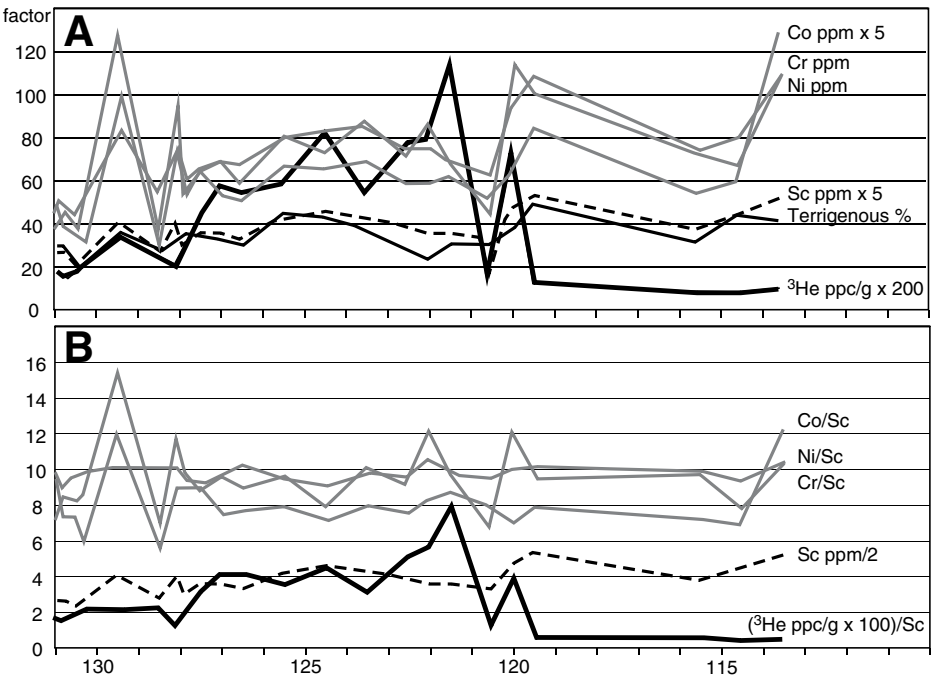

Figure 4. (A) Stratigraphic plot comparing the abundance of extraterrestrial ^{3}He (in 10–12 cm^3 per gram of bulk sample [ppc/g]), terrigenous component (siliciclastic + C_{org}), scandium (terrigenous), and possibly chondritic nickel, cobalt, and chromium through the Monte dei Corvi Beach section. (B) Plot of the ratios of ^{3}He, Ni, Co, and Cr over Sc.

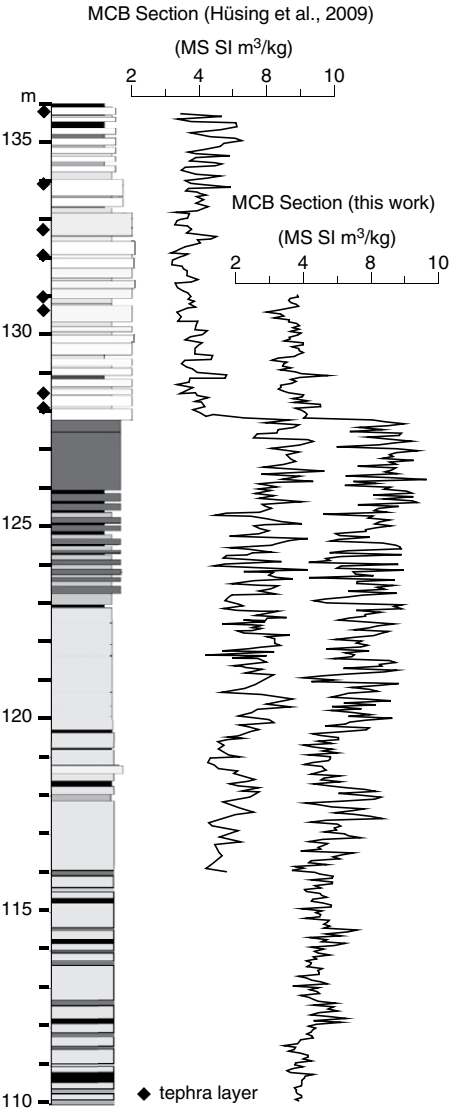

Figure 5. The Monte dei Corvi Beach (MCB) magnetic susceptibility (MS) series of Hüsing et al. (2009) compared to the one measured at 5 cm resolution in the same section for this work.

Downloaded from https://pubs.geoscienceworld.org/gsa/gsabulletin/article-pdf/129/9-10/1357/2615686/1357.pdf
by University of Western Ontario user

Calcium Carbonate

The overall $CaCO_3$ weight percent profile shown in Figure 3C exhibits variations that mimic fairly well the differences among the various lithostratigraphic members. Up to meter level 117.6, carbonate content in what Hüsing et al. (2009) visually defined as gray marls, varies between 45 wt% and 73 wt%. This indicates that they are, technically speaking, marls and calcareous marls. On the other hand, more or less distinct (i.e., relatively more or less dark) sapropels have generally lower carbonate content down to ~37 wt%, and so they can also be defined as marls, although they may vary in composition independently from their more-or-less-dark visual appearance. For instance, some distinct sapropels, like those at 110.10 m, 112.65 m, 114.60 m, and 116.00 m, have $CaCO_3$ compositions varying between 50 and 62 wt%, whereas the barely visible sapropel at meter level 115.70 has a composition as low as 37 wt%.

At 117.6 m, the mean $CaCO_3$ composition drops down from ~60 wt% to ~50 wt% up to 120.0 m. Within this interval, a couple of layers at 118.7 m have a composition rising back up to ~60 wt%, whereas a prominent sapropel at 118.35 m has a carbonate composition of 38 wt%. Three other thin sapropelic horizons varying from distinct to visible (according to the visual lithology of Hüsing et al., 2009) all have $CaCO_3$ compositions around 48 wt%. Then at 120.0 m, the carbonate profile shows another sharp positive shift of the mean composition, rising up to calcareous marls with 65 ± 5 wt% $CaCO_3$ all through the rest of the Marly Member.

With the beginning of the Brownish Member, mean carbonate composition drops again to ~55 wt% and then rises back up to ~60 wt% at 126.0 m through the upper, visually homogeneous part of the unit, where the mean composition returns around 62 wt%, with six distinct excursions of ±8 wt%. A slight increase in mean $CaCO_3$ composition around 66 wt% characterizes the lower part of the well-bedded Rossini Member, up to meter level 131.0.

LOI Organic Carbon

As expected, the concentration of organic carbon (C_{org}), as measured by LOI at 360 °C (Fig. 3E), yielded high values ranging between ~8 and 14 wt% in the sapropelic horizons logged by Hüsing et al. (2009), but the absolute value often does not reflect the visually estimated prominence. For instance, distinct sapropel at 113.7 m has about the same C_{org} abundance as the prominent sapropel at 114.3 m, but it has much more C_{org} than a visually defined distinct sapropel at 110.3 m. Moreover, some horizons (i.e., at meter levels 113.5, 115.1, 117.1, and 121.35) with relatively high C_{org} contents do not correspond to any visible sapropelic marl. On the other hand, prominent sapropel at 122.95 m yielded a relatively low C_{org} composition of ~4.5 wt%.

Carbon and Oxygen Stable Isotopes

The $\delta^{18}O$ and $\delta^{13}C$ profiles through the Monte dei Corvi Beach section are shown in Figures 3F and 3G, respectively. Both profiles exhibit a series of positive and negative shifts between 0.3‰ and 0.8‰, which are remarkably similar to shifts recorded in deep-sea calcareous benthos through the same time interval (i.e., between ca. 8.5 and ca. 7.3 Ma) by Zachos et al. (2001), and in time-equivalent records of terrestrial leaf wax (C_{31} *n*-alkene) δD and $\delta^{13}C$ from ODP Site 722 (Arabian Sea) of Huang et al. (2007), as shown in Figure 6. It is noteworthy to point out that $\delta^{18}O$ in the time interval across the Tortonian-Messinian boundary evolves in a long-term positive trend, as already defined in the La Sardella section by Montanari et al. (1997), in the oceanic record of Zachos et al. (2001), as well as in the δD of Huang et al. (2007), which suggest a gradual cooling of global climate. This general positive trend seems to be interrupted by a negative shift at ca. 8.7 Ma in the records of Zachos et al. (2001) and Huang et al. (2007), and then it is followed by an interval of brief shifts up to ca. 7.2 Ma, where these profiles resume their general positive trend all through the early Messinian. The same relevant shifts are also recorded in the Monte dei Corvi Beach section at meter level 117.5, ~2 m below the inception of the ^3He anomaly (see Figs. 3B and 6). Similarly, the $\delta^{13}C$ value, which exhibits a general negative trend (Zachos et al., 2001) in the oceanic deep-sea record through the same mid-Tortonian to mid-Messinian time interval (and also in the La Sardella section; Montanari et al., 1997), shifts quickly in a negative sense by as much as 0.6‰ at around 8.6 Ma. This negative shift of the $\delta^{13}C$, which interrupts the general positive trend through the Tortonian-Messinian time interval, is also recorded in the terrestrial leaf wax series of ODP 722 in the northwestern Indian Ocean (Huang et al., 2007; see Fig. 6).

In summary, the $\delta^{18}O$ and $\delta^{13}C$ stable isotope record in the Monte dei Corvi Beach section shows trends and shifts similar to stable isotopes in the global deep-sea record and the terrestrial plant record of southwestern Asia through the same time interval. An important negative shift at 117.5 m in both stable isotope records preceded the inception of the ^3He anomaly by ~2 m, and it is followed by an interval of rapid trend shifts lasting through the whole stratigraphic interval with elevated ^3He. This suggests a possible link between the Veritas event and global climatic and environmental changes.

MULTIPROXY CYCLOSTRATIGRAPHIC ANALYSIS: RESULTS AND INTERPRETATIONS

The five high-resolution proxy series through the Upper Tortonian Monte dei Corvi Beach section provide the basis for a spectral cyclostratigraphic analysis via FFT, which is aimed at assessing whether or not these pelagic sediments have recorded global climatic changes, and also local environmental changes induced by orbital cycles, i.e., the so-called Milankovitch cycles (eccentricity, tilt or obliquity, and precession [ETP]). As seen from a different perspective, these proxy series may not record regular or rhythmic changes, but they may instead reflect environmental changes induced by local random phenomena such as regional volcanism and/or tectonics, or possibly atmospheric perturbations provoked by extraterrestrial events such as impacts or, as in our Veritas case, an exceptional influx of extraterrestrial matter following an asteroidal breakup.

The results of the spectral analysis for each proxy series are illustrated individually in Figure 7, and therein compared with the FFT outputs of the ETP solution of Laskar et al. (2004) through the Tortonian–early Messinian time interval from 11.5 to 6.5 Ma, including the resulting June insolation as calculated for a northern latitude of 65° (Figs. 7A1 and 7A2).

Magnetic Susceptibility (MS) Series

The upper 3 m of the MS series was normalized to the mean of the fairly linear record of the lower part of the section in order to eliminate the effects on the power spectrum of the sharp negative shift of the mean MS intensity measured through the Rossini Member (see Fig. 5). In other words, this was done to prevent a strong low-frequency component from overwhelming the power spectrum and thus dampening the relative power of higher-frequency components. Both periodogram and sliding window spectra exhibit four significant components reaching or surpassing the 95% C.L., with stratigraphic wavelengths of A = 23.7 cm, B = 48.3 cm, C = 109.6 cm, and D = 475 cm (Figs. 7B1 and 7B2). The ratios of frequency period A to the other frequency components of the periodogram in the stratigraphic domain, i.e., A/B = 0.491, A/C = 0.216, and A/D = 0.050, are very similar to the ratios of the mean precession (P = ~21 k.y.) over the tilt (T = ~41 k.y.), the mean short eccentricity (SE = ~100 k.y.), and the mean long eccentricity (LE = ~400 k.y.) from the ETP solution of

Downloaded from https://pubs.geoscienceworld.org/gsa/gsabulletin/article-pdf/129/9-10/1357/2615686/1357.pdf
by University of Western Ontario user

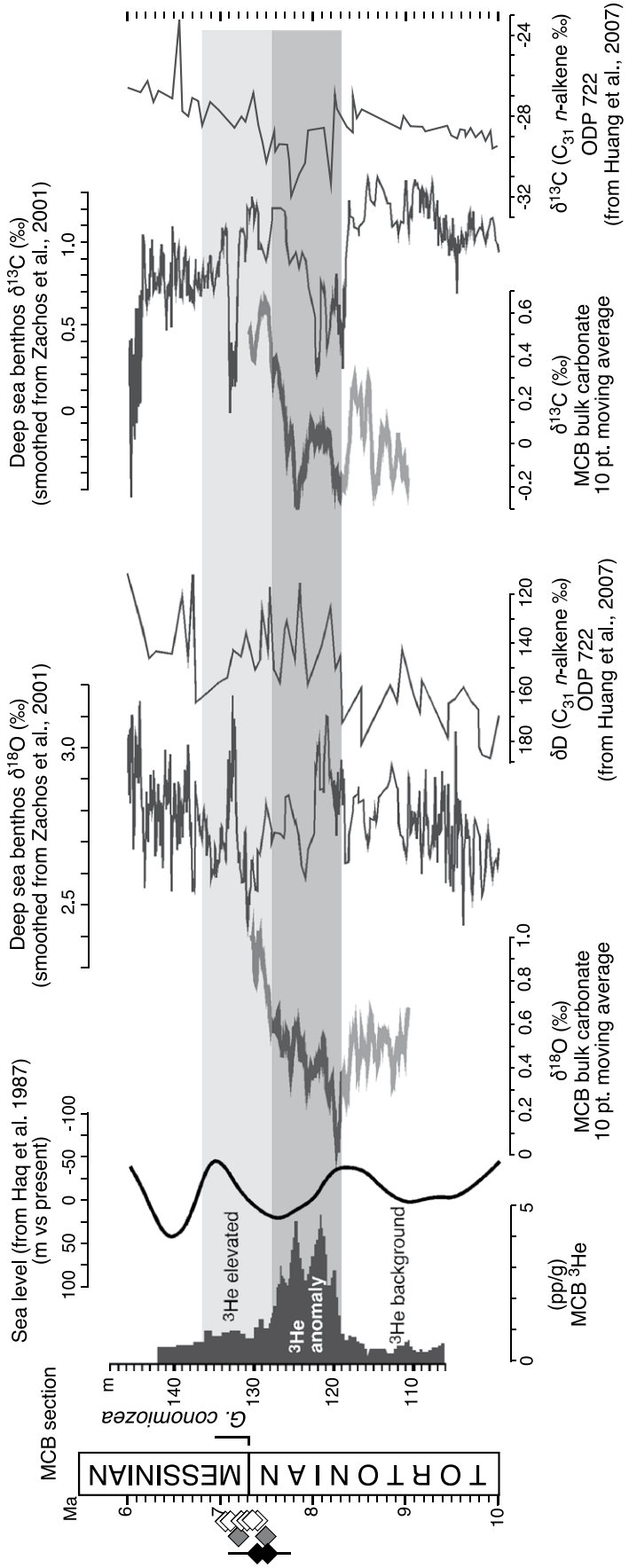

Figure 6. Correlation between the Tortonian-Messinian oceanic and continental oxygen and carbon stable isotope records, and those of the Monte dei Corvi Beach (MCB) section. ^{3}He is given in 10–12 cm^3 per gram of bulk sample (pp/g). ODP—Ocean Drilling Program; *G.—Globorotalia*.

Laskar et al. (2004) shown in Figure 7A1, i.e., P/T = 0.512, P/SE = 0.210, and P/LE = 0.052. This suggests that the main frequency components of the MS proxy series from the Monte dei Corvi Beach section represent ETP Milankovitch cycles. By migrating this MS stratigraphic series into a time series using a conversion function in the MATLAB routine, a mean sedimentation rate of 11.8 m m.y.$^{-1}$ was obtained (Fig. 7B1). This inferred mean sedimentation rate for the uppermost Tortonian Marly Member–Brownish Member interval is consistent with estimates of the sedimentation rate for the Schlier Formation, which, in the composite Monte dei Corvi section, decreases from a mean of ~37.7 m.y.$^{-1}$ through the 49-m-thick Serravallian Calcareous Member (Cleaveland et al., 2002) to a mean of 15.7 m.y.$^{-1}$ through the Lower Tortonian Marls-Sapropels Member, between the base of chron5Cn and the top of chron C4An (Hüsing et al., 2007).

The precession signal is both relatively powerful and stationary, with just a barely perceptible, gradual shift toward higher frequencies in the lower half of the section, suggesting a slight decrease in mean sedimentation rate, and a clearer shift to lower frequencies in the uppermost part of the section. This indicates a slight increase of sedimentation rate in the Rossini Member. Next, we verified whether or not the precession component bears an amplitude modulation by eccentricity, as one expects from astronomical theory. A Hilbert transform was performed on a precession band-pass, with a broad filter between 17 and 27 k.y. The power spectrum of the Hilbert amplitude demodulated signal was then compared to the power spectrum calculated for the Hilbert transform performed on the ETP series from Laskar et al. (2004). The MS Hilbert periodogram yielded weak frequency peaks compatible with ~100 k.y. short eccentricity frequencies, and a strong sharp peak at the expected frequency of ~405 k.y. long eccentricity. The Hilbert periodogram of the precession cycles, as recorded by MS, exhibits two other relatively powerful modulation peaks with periods of 141 and 196 k.y., which do not correspond to frequencies of precession modulation. They may represent noise contained in the MS series.

The imprint of obliquity appears somewhat blurred and less sharp than that of precession. Rather than a steady periodicity around 41 k.y., we observe shifts to higher frequencies through the lower part of the section, and to lower frequencies through the uppermost part of the section. As for the short ~100 k.y. eccentricity component, the peak with a period of 109.6 cm, equivalent to a period of 94.3 k.y. with a mean sedimentation rate of 11.8 m m.y.–1, is weak, barely reaching the 95% C.L. Yet, this frequency peak has the exact same period of 94.3 k.y. as the dominant short

Downloaded from https://pubs.geoscienceworld.org/gsa/gsabulletin/article-pdf/129/9-10/1357/2615686/1357.pdf
by University of Western Ontario user

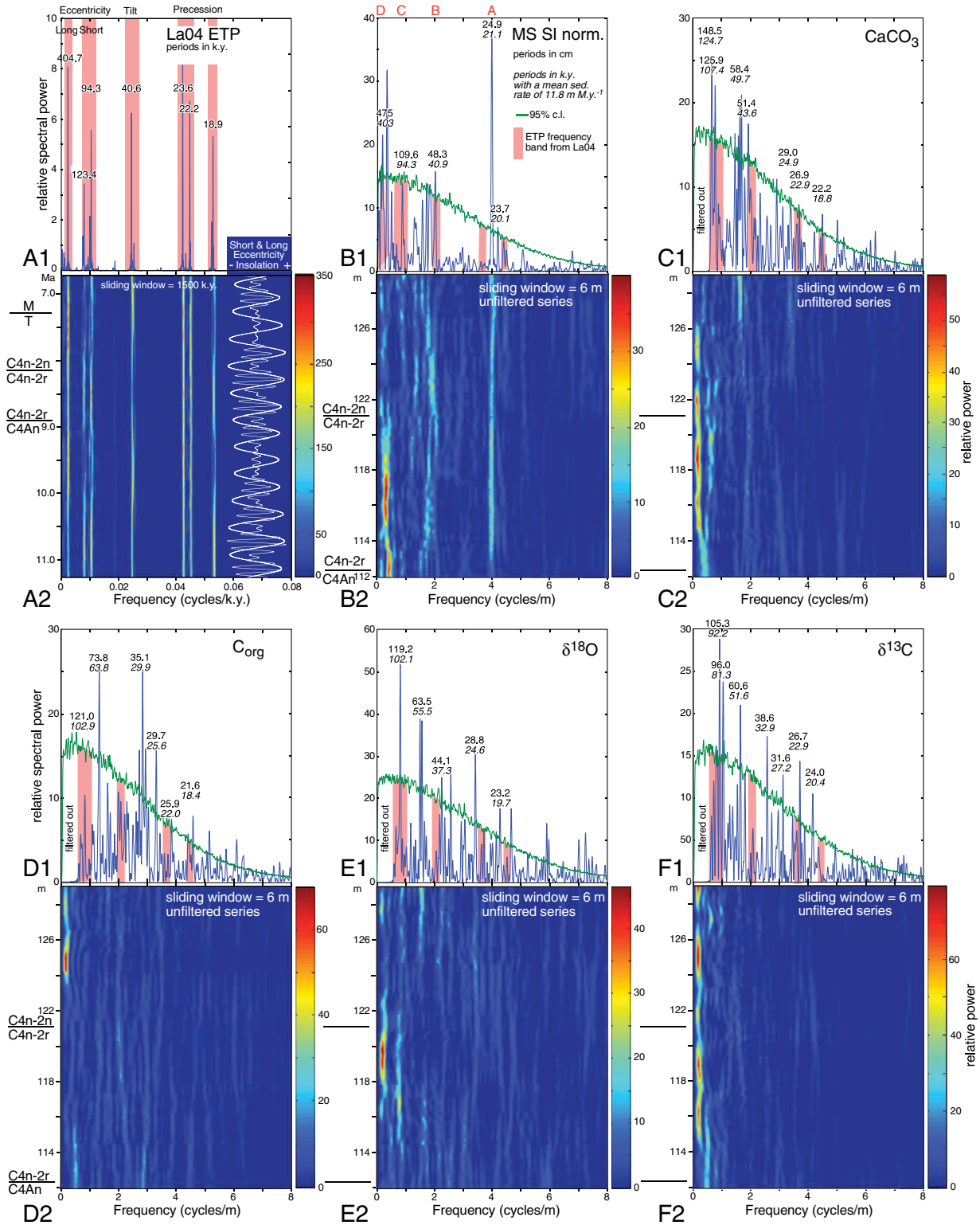

Figure 7. (A1–A2) Synoptic graphic plots of the eccentricity, tilt or obliquity, and precession (ETP) solution of Laskar et al. (2004; La04 in the figure) for the Tortonian (T) to Messinian (M) time interval from 10.5 to 6.5 Ma compared to the fast Fourier transform (FFT) cyclostratigraphic syntheses for the Monte dei Corvi Beach section of magnetic susceptibility (MS) (B1–B2), $CaCO_3$ (C1–C2), loss on ignition (LOI) C_{org} (D1–D2), $\delta^{18}O$ (E1–E2), and $\delta^{13}C$ (F1–F2) proxy series (c.l.—confidence level). Red uppercase letters A, B, C, and D in plot B1 indicate the positions of the frequency peaks here interpreted respectively as precession, tilt, short eccentricity, and long eccentricity (see text for explanation). In all the sliding window FFT outputs (A2, B2, C2, D2, E2, and F2), the stratigraphic positions of chronal boundaries are annotated.

Downloaded from https://pubs.geoscienceworld.org/gsa/gsabulletin/article-pdf/129/9-10/1357/2615686/1357.pdf
by University of Western Ontario user

eccentricity frequency of Laskar et al. (2004). In the periodogram of the MS series in Figure 7B1, a sharp and powerful peak emerges well above 95% C.L. at a period of 475 cm, equivalent to a period of 403 k.y. in the time domain, which likely represents the ~405 k.y. long eccentricity cycle. This signal is particularly strong in the lower part of the Monte dei Corvi Beach section, up to meter level 119, as seen in the sliding window FFT output in Figure 7B2. A Hilbert test for short eccentricity yielded FFT power spectra dominated by strong power in the low frequencies, masking the higher-frequency spectral peaks, which suggests a strong amplitude modulation of the short eccentricity cycle by the expected frequency of ~405 k.y. representing the long eccentricity cycle.

In summary, a spectral analysis of the high-resolution MS series reveals significant frequencies (exceeding the 95% C.L.) consistent with the ETP frequencies predicted by Laskar et al. (2004), notwithstanding the fact that this series bears some degree of noise. This suggests that the influx of terrigenous (magnetic) material into the Umbria-Marche synorogenic pelagic basin was mainly controlled by wet-dry, orbitally forced climatic cycles affecting the source area, presumably the midlatitude Alpine orogen, from which fine-grained magnetic material contained in the soil was washed out by the runoff preferentially during soil-forming wet (and presumably warm) periods.

Calcium Carbonate Series

The calcium carbonate ($CaCO_3$) series yielded FFT power spectra dominated by strong low-frequency signals, which mask the higher-frequency signals (see sliding window output in Fig. 7C2). To overcome this problem and search for possibly significant signals in the broad band of ETP frequencies, a FFT was performed on the data series filtered with a band-pass of 0.1–1.6 m, as an attempt to eliminate the effect of overwhelming very low frequencies, and thus focus on the higher-frequency components of this proxy. The periodogram of the filtered series in Figure 7C1 still shows a noisy spectrum of frequencies, out of which only weak signals in the high-frequency band with periods of 22.2 and 26.9 cm could be ascribed to precession cycles. Other than these, relatively strong signals in the frequency band with periods of 50–60 cm (44–50 k.y. in the time domain) do not quite match the tilt cycle with a predicted period of ~41 k.y., whereas strong signals with periods of 126–148 cm (107–125 k.y. in the time domain) are fairly close to the periods for short eccentricity of ~94–123 k.y. as calculated by Laskar et al. (2004). A Hilbert test of the $CaCO_3$ presumed precession band revealed a weak amplitude modulation by eccentricity. However, we could not detect an amplitude modulation of the ~100 k.y. short eccentricity cycles, which we directly filtered from the $CaCO_3$ record, by the ~400 k.y. long eccentricity cycle (Fig. 8B2).

In principle, the calcium carbonate content in these pelagic sediments should be, to a certain degree, inversely proportional to the terrigenous (insoluble and magnetic) component, so it seems unusual that the spectrum of the $CaCO_3$ series differs so strongly from the MS spectrum. In the Serravallian Monte dei Corvi section, for instance, which represents a clear pelagic limestone-marl rhythmite successfully tuned to the eccentricity cycle by Cleaveland et al. (2002) on a statistical basis, $CaCO_3$ compositions of 354 individual samples collected at 5 cm intervals (from Cleaveland, 2001; see raw data in Table DR4 in the GSA Data Repository [see footnote 1]) correlate inversely with MS intensity, with a significant R^2 coefficient of 0.549. The stratigraphic variation in the correlation between the MS and $CaCO_3$ here was examined using a 4 m sliding widow calculation of the p value correlation coefficient through the section, which revealed an excellent correlation between 0.5 and 1.0×10^{-4} (Fig. 9A). Band-pass curves of the Monte dei Corvi data with a broad filter encompassing the precession frequency band (i.e., 17–27 k.y.), show an almost perfect antiphase correlation between the MS and $CaCO_3$ series, as well as corresponding amplitude variations, as one might expect (Fig. 9B). On the contrary, the 420 samples collected through the 21-m-thick Monte dei Corvi Beach section (Fig. 10A) have a variable R correlation coefficient for the 4 m sliding window calculation that is generally negative through most of the section (as one may expect) but positive in the intervals comprising the main peaks of ^3He concentration. As for an estimate of correlation between the two series, p values >0.1 in the intervals comprising the main peaks of ^3He concentration suggest poor (i.e., statistically insignificant) correlation. Through the lower 8 m of the section, the MS and $CaCO_3$ eccentricity band-pass curves show a fairly consistent antiphase relation of cycles 1–7, as one may expect (Fig. 10A), but then, through the following ^3He interval, cycles 9–17 are either off-phase or in-phase. A return to an antiphase relation is observed in the Rossini Member, at the top of the section and out of the ^3He interval.

In summary, cyclostratigraphic spectral analysis of the high-resolution $CaCO_3$ proxy series through the Monte dei Corvi Beach section leads to the perception that, unlike the MS series, this proxy series does not bear a strong imprint from astronomical components. This could suggest that the ETP forcing is blurred by some random external forcing mechanism affecting the local primary plankton carbonate production relative to the distal influx of hemipelagic terrigenous material.

Organic Carbon Series

The organic carbon content in the Monte dei Corvi Beach section is generally higher in dark sapropelic marls than in gray calcareous marls (see Fig. 3E), where sapropels reflect moments of reducing conditions on the seafloor that allowed for the preservation of organic matter. Changes in these environmental conditions on the seafloor may well be controlled by changes in the climate affecting the Umbria-Marche Basin, such as vertical mixing, as opposed to stagnation of deep-marine waters and/or eutrophication of superficial waters with consequent excess production of organic matter. Nevertheless, slight undulations of the paleoseafloor topography, as in the example of the Upper Cenomanian Scaglia Bianca Formation (Beaudoin et al., 1996), may cause reducing conditions in depocenters, with consequent localized accumulation of sapropelic sediment, and more oxidizing conditions on relatively higher, winnowed parts of the seafloor, which would prevent preservation of organic matter (M'Ban, 1996).

The rhythmic alternation of gray calcareous marls and dark sapropelic marls in the Lower Tortonian Marls-Sapropels Member was interpreted by Hüsing et al. (2007, 2009) as the expression of the precession cycle where more or less dark sapropelic marls represented maxima in insolation, as opposed to gray calcareous marls, which represented insolation minima. This interpretation would allow for the astronomical tuning of the lithologic series with the astronomical solution of Laskar et al. (2004). However, in the upper part of the Monte dei Corvi Beach section, which includes the Marly, Brownish, and Rossini Members, sapropelic layers are rare, rendering tuning on visual lithologic inspection difficult, if not impossible. Aware of all this, we performed a FFT spectral analysis of a high-resolution series of the total organic carbon content of the Monte dei Corvi Beach section as obtained from LOI of powdered dry samples at 360 °C (Figs. 7D1 and 7D2). Similar to the results for $CaCO_3$, the C_{org} series yielded FFT power spectra overwhelmed by relatively strong low-frequency power, masking higher-frequency signals (Fig. 7D2). Despite filtering the series with a broad band-pass of 0.1–1.6 m, the periodogram in Figure 7D1 still shows an overall noisy spectrum. We observe spectral peaks exceeding the 95% C.L. in the high-frequency band that are compatible with precession. However, equally strong peaks have periods of 29.7, 35.1, and 73.6 cm and cannot be ascribed to any of the Milankovitch

Downloaded from https://pubs.geoscienceworld.org/gsa/gsabulletin/article-pdf/129/9-10/1357/2615686/1357.pdf
by University of Western Ontario user

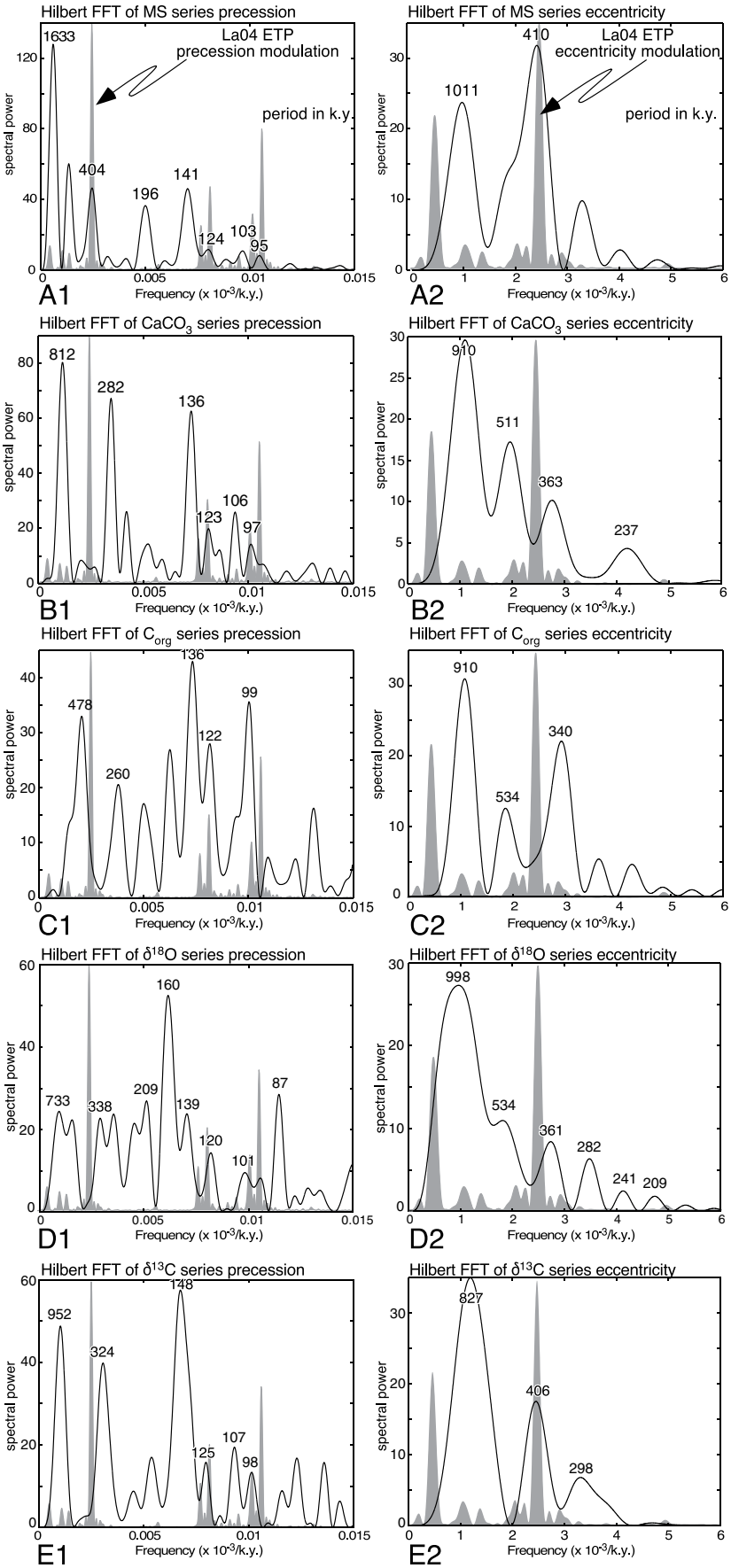

astronomical parameters. No significant signals above noise level are found in the short eccentricity band. A Hilbert test of the C_{org} presumed precession band reveals a strong modulation by ~100 k.y. short eccentricity, and possibly also by ~405 k.y. long eccentricity. However, no modulation of the filtered (85–150 k.y.) short eccentricity cycles by long eccentricity can be deduced from Figure 8C2.

A sliding window *p* value test of the MS versus the C_{org} series (Fig. 10B) indicates poor correlation between the two series through most of the section, with just a few intervals, i.e., 113.0–114.5 m, 120.5–124.0 m, and 126.5–127.5 m, having a significant *p* value <0.1 and positive *R* coefficient. Surprisingly, not even the apparently rhythmic Marls-Sapropels Member in the lowermost part of the section bears any statistically significant correlation between the two series.

A comparison between the eccentricity bandpass curve of the MS series (filter of 1.0–1.8 m) and that of the C_{org} series reveals a consistent antiphase relation through the Rossini Member, an in-phase relation through most of the ^{3}He interval (i.e., from 122 to 127 m), and inconsistent phase relations through the pre-Veritas, lower part of the section (Fig. 10B). This suggests that organic matter through the Rossini Member was preserved on the seafloor preferentially in times of low terrigenous influx or high calcareous plankton production, equivalent to dry and possibly cold orbitally forced periods (i.e., eccentricity minima). On the contrary, through the ^{3}He interval, the opposite seems to have occurred: relatively reducing conditions on the seafloor leading to preservation of relatively high concentrations of C_{org} during wet and possibly warm periods. As for the part of the section preceding the ^{3}He anomaly, no consistent relation seems to exist between orbitally forced climatic changes and accumulation of C_{org} on the seafloor. More specifically, in the interval 110–116 m, which expresses the characteristic rhythmic alternation of sapropels and calcareous marls of the Sapropels-Marls Member, cycles 3, 4, and 5 show an antiphase relation between the MS and C_{org} series, whereas cycles

Figure 8. Hilbert fast Fourier transform (FFT) outputs for the precession and short eccentricity from the eccentricity, tilt or obliquity, and precession (ETP) solution of Laskar et al. (2004; La04 in the figure) compared to those for the Monte dei Corvi Beach section magnetic susceptibility (MS) (A1–A2), $CaCO_3$ (B1–B2), loss on ignition (LOI) C_{org} (C1–C2), $\delta^{18}O$ (D1–D2), and $\delta^{13}C$ (E1–E2) proxy series.

Downloaded from https://pubs.geoscienceworld.org/gsa/gsabulletin/article-pdf/129/9-10/1357/2615686/1357.pdf
by University of Western Ontario user

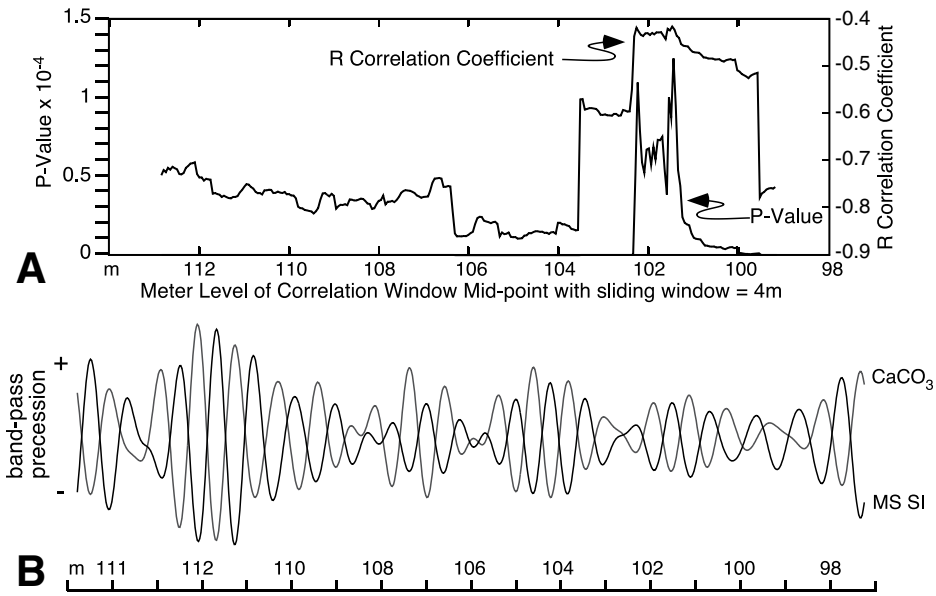

Figure 9. (A) Plot of a 4 m sliding window calculation of the *R* correlation coefficient and *p* value of the $CaCO_3$ vs. magnetic susceptibility (MS) for 5-cm-resolution series from the lower Serravallian Calcareous Member of the Schlier Formation in the Monte dei Corvi section analyzed by Cleaveland (2001) and Cleaveland et al. (2002). (B) Precession-filtered band-pass curves for the $CaCO_3$ and magnetic susceptibility (MS) series from the same Monte dei Corvi section.

1 and 2 show off-phase and in-phase relations, respectively (Fig. 10B). In summary, the FFT spectral analysis of the C_{org} series suggests that orbitally forced climatic changes were not the sole cause of environmental changes in the deep sea in this part of the western Tethyan Ocean during the latest Tortonian, when incipient restriction of the Mediterranean Sea may have affected efficient mixing with the global ocean.

Oxygen Isotope Series

In a global glacio-eustatic climatic system, such as the one of the late Miocene, the isotopic composition of oceanic water expressed by $\delta^{18}O$ is the most direct signature of Milankovitch climatic oscillations, where relatively high $\delta^{18}O$ in marine biogenic carbonate indicates glacial periods (i.e., cold and generally dry) and vice versa, i.e., relatively low $\delta^{18}O$ indicates interglacial periods (i.e., warm and wet). In a glacio-eustatic system, relatively warm and wet periods in the Northern Hemisphere occur at precession and eccentricity maxima, whereas cold climate conditions occur at precession and eccentricity minima. Therefore, a $\delta^{18}O$ proxy series from a Tethyan marine pelagic carbonate succession is expected to record cyclic excursions with periods compatible with orbital precession and eccentricity frequencies.

Through the Monte dei Corvi Beach section, the $\delta^{18}O$ proxy series yielded noisy spectra dominated by low-frequency signals (Fig. 7E2), The filtered periodogram in Figure 7E1, which was meant to eliminate the effect of overwhelming very low frequencies and highlight the higher-frequency components in the ETP band, shows a most powerful and rather stationary signal with a period of 119.2 cm (102.2 k.y. in the time domain, given our assumed sedimentation rate of 11.8 m m.y.–1), compatible with short eccentricity. Powerful signals with periods of 28.8 cm (= 24.6 k.y.) and 23.2 cm (= 19.7 k.y.), are close to precession frequencies, whereas a weak signal with a period of 44.1 cm (= 37.3 k.y.) is close to, but not quite, the expected frequency of ~41 k.y. of obliquity. A strong signal with a period of 63.5 cm (= 55.5 k.y.) may represent noise contained in the $\delta^{18}O$ series. The periodogram of a Hilbert transform for the precession band shows weak frequency peaks with periods of ~101 and 120 k.y. (Fig. 8D1), which suggest a weak eccentricity modulation. However, the same Hilbert test for the eccentricity band produces a peak with a period of 361 k.y., which is close to, but not quite, the expected long eccentricity frequency of ~405 k.y. (Fig. 8D2).

A sliding window correlation between the MS and the $\delta^{18}O$ series (Fig. 10C) reveals a relatively high coefficient of negative correlation in the Rossini Member, indicating that samples with a high $\delta^{18}O$ have a low magnetic terrigenous component (or a relatively high biogenic carbonate component), as one may expect. The same is observed in the lower part of the section up to meter level 114. Through the central part of the Monte dei Corvi Beach section, which comprises the ^3He anomaly, the correlation between MS and $\delta^{18}O$ switches to positive values, but *p* values through the intervals 114.0–119.5 m and 122.0–126.5 m are greater than 0.1, indicating poor or no statistically significant correlation.

A comparison between the eccentricity band-pass curve of the MS series and that of the $\delta^{18}O$ series reveals an almost consistent antiphase relation through most of the section, with the exception of in-phase cycles 9 and 10 in the upper part of the massive Marly Member, which correspond to the lower part of the ^3He anomaly (Fig. 10C). Assuming that maxima in MS correspond to maxima in short eccentricity (warm and wet climate conditions), the antiphase relation between the two proxy series is what one might expect considering that high $\delta^{18}O$ is indicative of global glacial conditions in a glacio-eustatic climate system. Therefore, the in-phase cycles 9 and 10 are suggestive of an anomalous climatic event, which happens to have occurred at the beginning of the abnormally high influx of extraterrestrial ^3He-rich interplanetary dust particles.

Carbon Isotope Series

The $\delta^{13}C$ signature in marine carbonates reflects the complex interplay of biological, sedimentological, and physical-chemical factors influencing the primary organic carbon productivity. Living organisms take up 12C easier than the heavier 13C, so they get enriched in 12C compared with the global availability in nature. Consequently, the $\delta^{13}C$ signal gives information about the carbon cycle, which is itself the result of a number of factors, such as biological productivity on land and in the oceans, weathering rates, oceanic circulation, carbonate cycle, and the relationship with pCO_2 in the atmosphere (e.g., Wendler, 2013). In general, it can be said that in the open-ocean domain, carbon isotopic fractionation is controlled by global climatic conditions, which vary through time in response to orbitally forced, and thus cyclic, climate changes. However, the orbital cyclicity of the $\delta^{13}C$ signature in a marine carbonate succession may be blurred or in any case altered in basins that are poorly connected with the open-ocean domain, and/or that are strongly influenced by the influx of terrigenous material derived from surrounding tectonically active orogens, as is the case for the late Miocene Umbria-Marche Basin. In fact, the $\delta^{13}C$ proxy series from the Monte dei Corvi Beach section yielded noisy spectra dominated by very low-frequency signals just as for the $\delta^{18}O$ series, whereas a filtered periodogram managed to

Downloaded from https://pubs.geoscienceworld.org/gsa/gsabulletin/article-pdf/129/9-10/1357/2615686/1357.pdf
by University of Western Ontario user

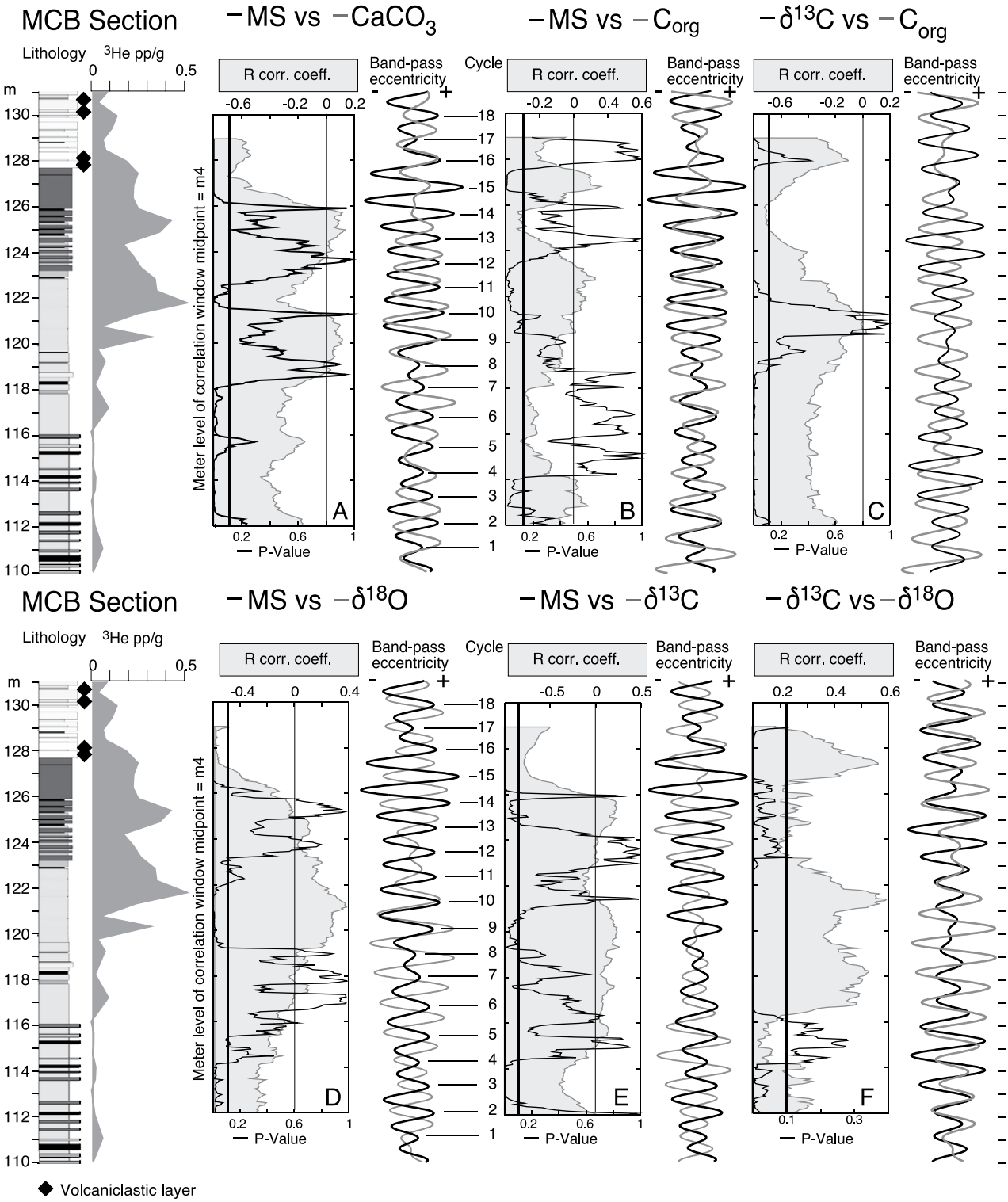

Figure 10. Cross-correlation of the (A) magnetic susceptibility (MS) vs. $CaCO_3$, (B) magnetic susceptibility (MS) vs. C_{org}, (C) $\delta^{13}C$ vs. C_{org}, (D) magnetic susceptibility (MS) vs. $\delta^{18}O$, (E) magnetic susceptibility (MS) vs. $\delta^{13}C$, and (F) $\delta^{13}C$ vs. $\delta^{18}O$ proxy series in the Monte dei Corvi Beach (MCB) section. ^3He is given in 10–12 cm^3 per gram of bulk sample (pp/g). Lithology patterns and shadings as in Fig. 2.

Downloaded from https://pubs.geoscienceworld.org/gsa/gsabulletin/article-pdf/129/9-10/1357/2615686/1357.pdf
by University of Western Ontario user

highlight higher-frequency components referable to the precession band, and a relatively strong signal with a period of 105.3 cm (92.2 k.y. in the time domain) possibly representing short eccentricity, which seems to be more evident in the lower and upper parts of the section (Figs. 7F1 and 7F2). A Hilbert test for the presumed precession band shows weak frequency peaks with periods of ~98 and 125 k.y. (Fig. 8E1), which suggest a weak short eccentricity modulation, whereas a strong signal with a period of 406 k.y. from a Hilbert test for the short eccentricity band reveals the expected amplitude modulation referable to long eccentricity (Fig. 8E2).

A sliding window correlation between the MS and the $\delta^{13}C$ series reveals poor or no correlation throughout most of the section from 114.5 m up to 126.5 m, with a positive *R* coefficient (Fig. 10D), and significant negative correlation with *p* values <0.1 in the intervals 112.5–114.5 m (upper part of the Marls-Sapropels Member), 120.0–121.5 (inception of the ^3He anomaly), and 126.5–129.5 m (comprising the homogeneous upper part of the Brownish Member and the lower part of the Rossini Member).

As for a comparison of the eccentricity band-pass curve of the MS series with the $\delta^{13}C$ series, cycles 1–7 (the pre-^3He interval) and cycles 17 and 18 (the post-^3He Rossini interval) are in antiphase relation. This suggests that in high-eccentricity periods (warm and wet climatic conditions), the availability of 12C in seawater was higher than in low-eccentricity periods, whereas through the rest of the section containing the ^3He anomaly, the cycles have variably in-, anti-, or off-phase relations (Fig. 10D).

It is interesting to note that the *p* value profile of MS versus $\delta^{13}C$ is very similar to the profile of $\delta^{13}C$ versus $\delta^{18}O$, and that the eccentricity band-pass curves between the two stable isotope series are almost consistently in an in-phase relation (Fig. 10E). All this indicates that the changes in these two stable isotope series through this late Tortonian time interval had a common forcing agent, which was acting not just in this part of the Tethys domain, but globally, if we consider the very similar pattern of negative and positive excursions recorded in deep-ocean series and in the continental series as well, as previously discussed and illustrated in Figure 6. However, that common forcing agent was not solely orbital climate forcing. As discussed already, we observed inconsistent phase relations between the isotopic proxies and MS throughout the ^3He interval. The MS series signal was interpreted to be mainly driven by orbital climate forcing, which suggests that the isotopic proxies experienced an additional driver throughout the ^3He interval. This additional climatic driver would thus be the cause of the observed inconsistencies in the relationship between the isotopic proxies and MS. It is also interesting to note that the *p* value profile of the $\delta^{13}C$ versus the C_{org} series (Fig. 10F) indicates a significant negative *R* correlation through most of the section, with the exception for the intervals 120.0–122.5 m (the first main ^3He anomaly), and 128.5–129.0 m (the base of the Rossini Member), where *p* values >0.1 indicate no statistically significant correlation. This suggests that the inception of these two nonoceanographic events, i.e., the anomalous influx of extraterrestrial ^3He and the Rossini volcanism, somehow altered the cyclic, climate-controlled carbon cycle affecting the Umbria-Marche pelagic basin.

ASTROCHRONOLOGIC DATING OF THE VERITAS EVENT

Among the five high-resolution proxy series through the Upper Tortonian Monte dei Corvi Beach section, only the MS series yielded FFT power spectra exhibiting stationary and statistically significant (95% C.L.) frequency signals referable to the precession, obliquity, and eccentricity cycles. All the other proxy series, including $CaCO_3$, C_{org}, $\delta^{18}O$, and $\delta^{13}C$, yielded noisy power spectra dominated by low-frequency signals, which dampened higher-frequency signals in the ETP band. Moreover, *p* value correlation and the comparison of eccentricity band-pass curves of the MS series with the other proxy series suggest that inconsistent relations exist, particularly in the middle part of the section, which is characterized by an enhanced concentration of extraterrestrial ^3He. Therefore, we attempted an astrochronologic tuning of the Monte dei Corvi Beach section using short and long eccentricity signals from the MS series correlated with the eccentricity from the solution of Laskar et al. (2004), as illustrated in Figure 11.

The Monte dei Corvi Beach section can be anchored to the chronostratigraphic time scale at the interpolated radioisotopic age of 7.3 ± 0.2 Ma for the Tortonian-Messinian boundary, as approximated by the first occurrence of planktonic foraminifer *G. conomiozea* by Vai (1997), Odin et al. (1997a), and Laurenzi et al. (1997). This chronostratigraphic boundary is found within the Rossini Member in the Sardella section (Montanari et al., 1997), which is located up high in the Monte dei Corvi cliff some 200 m to the northwest from the Monte dei Corvi Beach section, and would correspond approximately to meter level 132.5 in the Monte dei Corvi Beach section of Hüsing et al. (2007, 2009). U/Pb dating by Wotzlaw et al. (2014) of eight volcanosedimentary layers, which span the whole Rossini Member, yielded an age of 7.32 ± 0.02 Ma from zircons contained in a volcanosedimentary layer at meter level 132.46, thus consistent, within analytical uncertainty, with the Ar/Ar interpolated age of 7.3 ± 0.2 Ma for the Tortonian-Messinian boundary (e.g., Odin et al., 1997b, and references therein). This date corresponds, in the astrochronologic scale of Laskar et al. (2004), to a minimum of the long eccentricity cycle. The first long eccentricity minimum preceding the one at the Tortonian-Messinian boundary falls within the upper part of our Monte dei Corvi Beach section at about meter level 128.0. Here, two closely spaced U/Pb dates of Wotzlaw et al. (2014) bracketing meter level 128.0 yielded a mean age of 7.58 ± 0.02 Ma, thus ~100 k.y. younger than the astrochronologic age of 7.68 Ma for that long eccentricity minimum as calculated by Laskar et al. (2004) (see also Fig. 11). From there, four other long eccentricity minima, as determined from the FFT cyclostratigraphic analysis of the MS series, are recorded in the rest of the Monte dei Corvi Beach section. The inception of the ^3He anomaly, which we interpret as the chemostratigraphic signature of enhanced influx of ^3He-rich dust produced by the Veritas breakup, is located at about meter level 119.5, i.e., very close to a minimum of the long eccentricity band-pass derived from the MS proxy series. A fine-tuning with the trend of Laskar et al. (2004) for this stratigraphic level based on short and long eccentricity gives an astrochronologic age of 8.47 ± 0.05 Ma (Fig. 11), which is indistinguishable from, yet much more precise than, the age of 8.3 ± 0.5 Ma for the Veritas breakup as calculated by astrophysical means (Nesvorny et al., 2003). However, in the Monte dei Corvi Beach section, this ^3He positive shift postdates negative shifts of the oxygen and carbon isotopes by ~220 k.y., as well as a negative shift of the biogenic $CaCO_3$ (see Figs. 3 and 11). We interpret these shifts as the result of environmental changes caused by the impacts on Earth of Veritas-derived meteoritic material coarser than interplanetary dust particles, and therefore poor in ^3He, which would have been exhaled upon ablation while crossing the atmosphere (see following discussion). In this case, the actual Veritas breakup would have occurred at 8.69 ± 0.5 Ma.

DISCUSSION

The oxygen and carbon stable isotope records through the early Tortonian–early Messinian deep-sea benthos by Zachos et al. (2001), as well as those from terrestrial leaf δD and $\delta^{13}C$ from the Arabian Sea of Huang et al. (2007), reveal a change at ca. 8.5 Ma from a generally monotonic positive trend recorded until then through the late Miocene to a 1.3-m.y.-long period characterized by rapid trend shifts, which

Downloaded from https://pubs.geoscienceworld.org/gsa/gsabulletin/article-pdf/129/9-10/1357/2615686/1357.pdf
by University of Western Ontario user

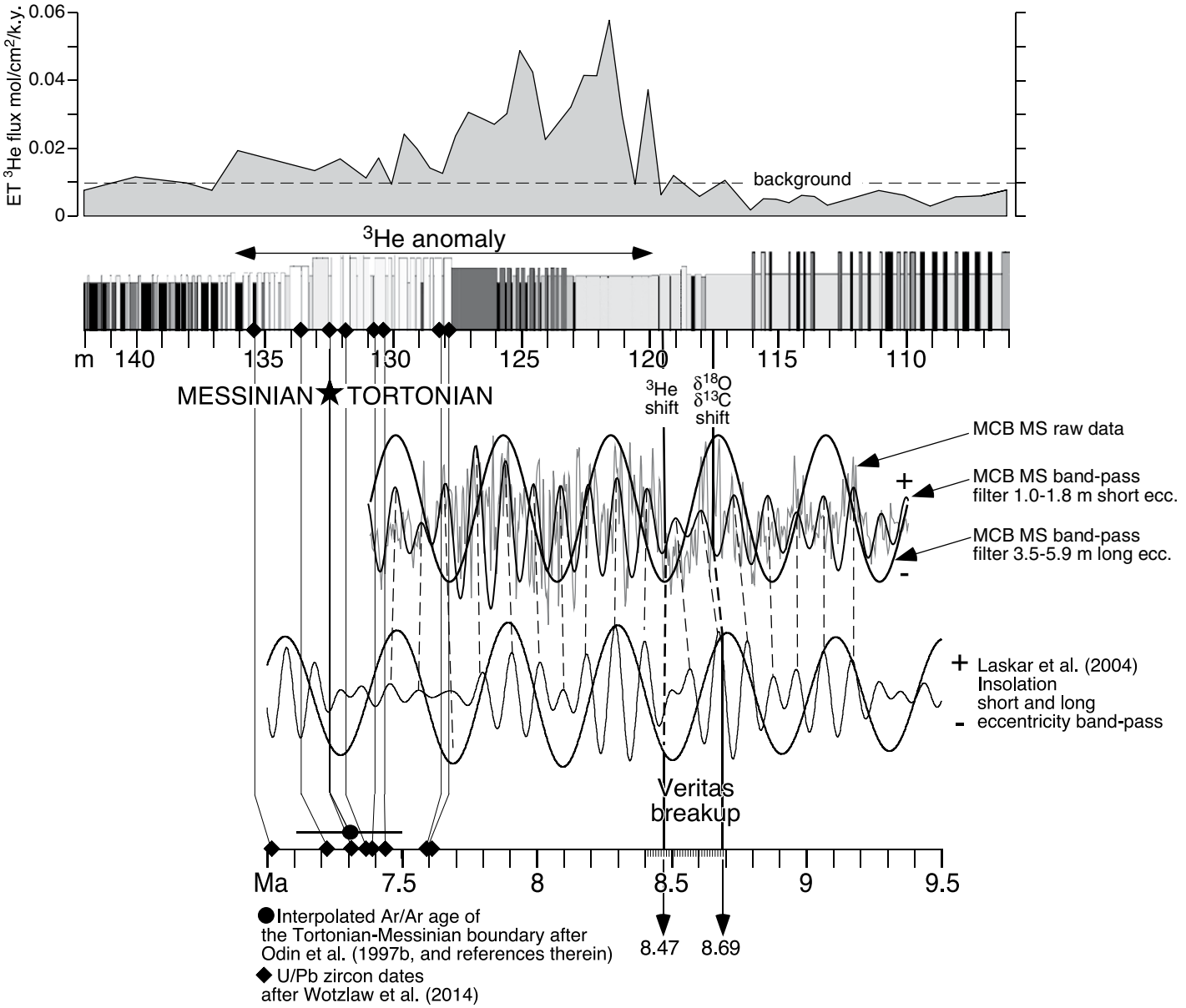

Figure 11. Synoptic graphic representation of the astronomical tuning of the Monte dei Corvi Beach (MCB) section, and astronomical age derivation for the inception of the Veritas ^{3}He interplanetary dust particle flux (ET—extraterrestrial) based on the long and short eccentricity (ecc.) insolation cycle from the solution of Laskar et al. (2004). MS—magnetic susceptibility.

suggest global climatic instability (see Fig. 6). In particular, sharp positive shifts in δ^{18}O of ~0.5‰ and in δD of ~45‰ point to a rapid cooling event between ca. 8.3 and ca. 8.0 Ma. A less pronounced positive shift is also found in the δ^{18}O and δD records between ca. 7.7 and ca. 7.4 Ma. The fact that similar brief δ^{18}O and δ^{13}C shifts are recorded in the Upper Tortonian Monte dei Corvi Beach section between 8.4 and 7.3 Ma (Fig. 6) suggests that this Tethyan pelagic succession records the same global climate changes inferred from the isotopic records of the open ocean (Zachos et al., 2001) and continental environments (Huang et al., 2007). Moreover, the alkenone SST record through the composite Monte dei Corvi–Monte dei Corvi Beach section of Tzanova et al. (2015) reveals a slight negative shift at 8.5 Ma, which denotes a gradual cooling of ~2 °C up to 7.6 Ma following a long time of relatively stable SSTs all through the underlying Serravallian and Lower Tortonian section. In addition to stable isotopes, our high-resolution cyclostratigraphic spectral analysis of environmental proxy series such as biogenic $CaCO_3$ and C_{org} suggest perturbations of orbitally forced climate cycles exactly through the interval with an enhanced influx of extraterrestrial ^{3}He, which serves as the chemostratigraphic telltale of a collisional event that created the Veritas family of asteroids (Farley et al., 2006, and references therein).

A similar situation, where Milankovitch cyclicity was disrupted or obscured through a pelagic carbonate succession with a prominent ^{3}He anomaly, was studied in the GSSP section for the Eocene-Oligocene boundary at Massignano by Brown et al. (2009). In that section, Farley et al. (1998) originally attributed the ^{3}He anomaly to a comet shower, whereas Tagle and Claeys

Downloaded from https://pubs.geoscienceworld.org/gsa/gsabulletin/article-pdf/129/9-10/1357/2615686/1357.pdf
by University of Western Ontario user

(2004) attributed it to an asteroidal bombardment. The presence of several impact structures of late Eocene age (see review by Koeberl, 2009) and the recent finding of extraterrestrial chromite grains belonging to two different meteorite types at the impact level of the Massignano section (Schmitz et al., 2015) support a multitype asteroid shower at this time period. In the case of Massignano, as in the case of the Upper Tortonian Monte dei Corvi Beach section, the MS series yielded FFT periodograms with clear ETP frequency signals, while the proxy series of $CaCO_3$, $\delta^{18}O$, and $\delta^{13}C$ did not show a cyclic organization through the ^3He anomaly. This was hypothesized by Brown et al. (2009) as possibly due to the fact that random (i.e., noncyclic) extraterrestrial events, such as comet or asteroid impacts, interacted with the continuous record of longer-term Milankovitch cycles in such a way that they were disrupted or obscured during the deposition of carbonate pelagic sediment (and thus the biogenic $CaCO_3$ and stable isotope records). Interplanetary dust incoming from an asteroidal breakup or a comet shower, or possibly the ejecta from a myriad of small meteorite impacts during such extraterrestrial events, may have altered the transparency of the atmosphere, causing global climate changes. On the other hand, the MS record, a proxy for the terrigenous influx, emerges largely unscathed, probably because this particular proxy would be less susceptible to climatic overprinting related to random extraterrestrial events than the other proxies. As suggested by Brown et al. (2009), the usual eluvial detrital influx is just slightly augmented by the slowly accreting extraterrestrial dust, and/or cold and warm spells would have affected the rhythmic, orbitally driven glacio-eustatic mechanism more than the wet-dry Milankovitch cycles affecting midlatitude continental areas, which are the source of the terrigenous (magnetic) influx in our Umbria-Marche Basin, thus giving to the MS proxy series a chance of preserving some level of cyclicity.

If the apparent coincidence of isotopic shifts and obscured Milankovitch cycles suggests a causal relationship between the Veritas event and local environmental and global climatic changes in a broad view, at a finer scale of observation, this coincidence is not as straightforward as it may seem. In the $CaCO_3$ and stable isotope series, for instance, negative shifts are recorded at meter level 117.5, whereas the inception of the ^3He anomaly is found at 119.5 m (Figs. 3B, 3D, 3F, and 3G). Thus, there seems to be a delay of ~220 k.y. until the cascade of ^3He-rich interplanetary dust particles with respect to environmental and/or climatic changes. This delay would argue against a cause and effect relationship between the Veritas asteroidal breakup and consequent environmental and/or climatic changes. Nevertheless, a similar situation is found in the Lower Turonian pelagic section of the Bottaccione Gorge at Gubbio. Here, a 15-m-thick interval (equivalent to ~1.8 m.y. duration) with elevated concentrations of ^3He attributed to a comet or asteroid showers by Farley et al. (2012) is preceded, by ~170 k.y., by $\delta^{18}O$ and $\delta^{13}C$ shifts and excursions as they were determined in this section by Sprovieri et al. (2013). Stoll and Schrag (2000) originally recognized these mid-Turonian isotopic events in the Gubbio section of the Contessa valley, ~2 km west from the twin Bottaccione section, during 10-cm-resolution analysis of bulk carbonate samples. In either section, the initial $\delta^{13}C$ negative shift is much sharper and more pronounced than the $\delta^{18}O$ shift (Fig. 12). Despite uncertainties in the precise correlation of isotopic excursions, which were precisely located in the classic biostratigraphic section of Gubbio, and sea-level changes, which were chronologically determined by Haq et al. (1987) upon a somewhat rough planktonic foraminiferal

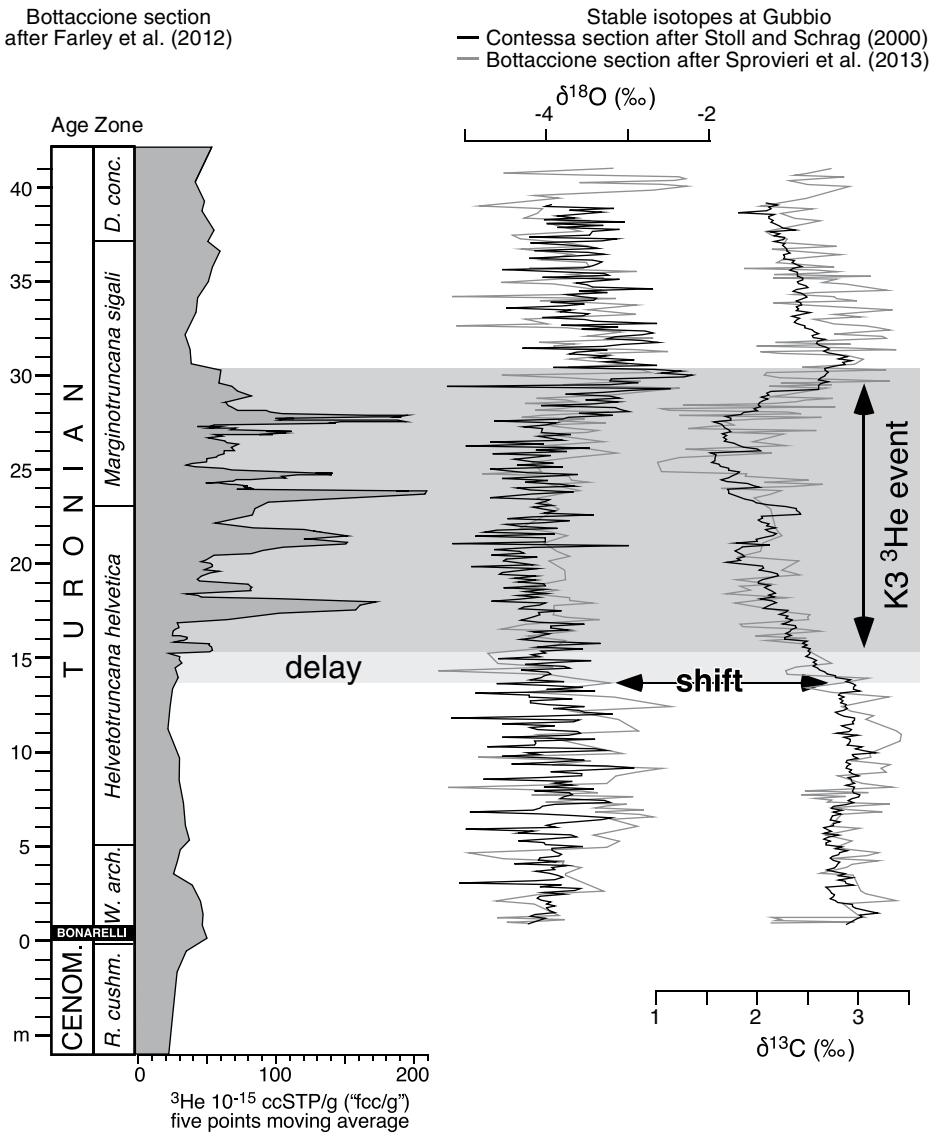

Figure 12. Correlation between the ^3He record (in cm^3/g at standard temperature and pressure [ccSTP/g]) of the Upper Cenomanian–Lower Turonian Bottaccione section and the oxygen and carbon isotopic record from the same stratigraphic interval in the Bottaccione and Contessa sections at Gubbio. Note that the unpublished $\delta^{18}O$ data from the Bottaccione section were kindly provided by Mario Sprovieri. Cenom.—Cenomanian. Planktonic foraminiferal biozones: *Rotalipoora cushmani, Whiteinella archeocretacea, Helvetotruncana helvetica, Marginotruncana sigali, Dicarinella concavata*. K3—mid-Turonian ^3He anomaly of Farley et al. (2012).

Downloaded from https://pubs.geoscienceworld.org/gsa/gsabulletin/article-pdf/129/9-10/1357/2615686/1357.pdf
by University of Western Ontario user

biochronology, Stoll and Schrag (2000) found the correspondence between the sea-level curve and the oxygen isotopic record of the Contessa section compelling (Fig. 12) and proposed that, in light of the correlation of regression events in the sea-level curve with positive oxygen isotopic excursions, there may be a link between climate and sea-level changes, possibly through control of sea level by buildup of continental ice sheets during episodes of climatic cooling. On the other hand, in light of the study by Farley et al. (2012), we found even more compelling the fact that these isotopic shifts and excursions coincide exactly with the interval showing an enhanced concentration of extraterrestrial ^{3}He. As documented here, a very similar situation is found in the Upper Tortonian Monte dei Corvi Beach section, where an elevated influx of ^{3}He-rich extraterrestrial matter persisted for ~1.6 m.y. Common sense would suggest that climate changes, with consequent environmental and sea-level changes, would not increase the influx of extraterrestrial matter, but the other way around is plausible, as suggested by Brown et al. (2009).

The question still to be answered is: Why, in both the cases of the mid-Turonian at Gubbio and the Upper Tortonian at Monte dei Corvi Beach, do the isotopic negative shifts, which indicate climate and/or environmental changes, predate the inception of the anomalous ^{3}He influx by as much as 170 or 220 k.y., respectively? The simplest, Occam's razor answer to this question is that in both cases, the extraterrestrial event occurred at a time when climate was already changing toward warmer conditions in response to background orbital forcing, thus giving a negative trend to the δ^{18}O signature independently from the actual extraterrestrial ^{3}He influx. On the other hand, it can be envisioned that the cascade of comminuted asteroidal matter initiated immediately after the breakup but prior to the arrival of an interplanetary dust particle mass large enough to leave a global ^{3}He signature. This initial cascade would contain a myriad of larger particles, from "shooting star"–size grains to larger, several-tens-of-meters–sized objects (similar to Chelyabinsk or Tunguska; cf. Farinella et al., 2001; Brown et al., 2013; Povinec et al., 2015), which, vaporizing in the atmosphere or upon impacting on the surface of Earth, would exhale their volatile ^{3}He content back to outer space and would not be massive enough to leave a detectable PGE signature worldwide. However, they may have been capable of causing an alteration of the atmosphere transparency, possibly triggering a climate change, which would be recorded by the δ^{18}O proxy with a short trend shift. This may explain the small δ^{18}O peak seen at 118.7 m in Figure 13. Within the interval with enhanced ^{3}He, the two main peaks at ~121.5 m and 124.5 m, as well as the minor peak at ~126.5 m, all coincide with maxima in the δ^{18}O record, i.e., the end of short positive trends (Fig. 13). The coincidence of these finer-scale isotopic shifts with the ^{3}He peaks not only suggests that the interplanetary dust particles (possibly associated with coarser asteroidal debris) cascaded in pulses after the Veritas breakup, but also that these accretionary pulses led to short cooling events.

The stratigraphic relationships among the ^{3}He, δ^{18}O, and SST records in the Monte dei Corvi section leads to a conundrum, a possible resolution for which requires a closer look at the available data. Tzanova et al. (2015) established a direct relationship between increasing aridity and significant cooling in the northern midlatitude circum-Tethyan region via high-resolution alkenone analysis through the composite Monte dei Corvi succession (from ca. 13 to ca. 6 Ma; see Fig. 2). The most prominent feature in this proto-Mediterranean SST curve is an episode of sharp cooling of as much 7 °C from a mean of ~26.5 °C, starting exactly at the base of the Rossini Member (ca. 7.7 Ma), which records an ~700 k.y. period of intense regional volcanism. This cooling event precedes the inception of the Messinian salinity crisis, which, in the Monte dei Corvi Beach section, is represented by the Euxinic Shales unit, followed by the mid-Messinian gypsum-sapropel rhythmite of the Gessoso-Solfifera Formation (e.g., Galeotti et al., 2010, and references therein). In the Euxinic Shales unit, the SST curve returns to values between ~24 °C and 26 °C, i.e., slightly cooler than the Tortonian mean of ~27 °C, evolving with a negative trend, which reflects the positive trend in the global oceanic δ^{18}O record of Zachos et al. (2001; see also Fig. 6). Through the Rossini Member, ^{3}He concentrations of ~0.1 pcm^3/g are a factor of 3–4 lower than those in the main anomaly interval between 119.5 m (ca. 8.5 Ma) and 127.5 m (ca. 7.7 Ma), but they are still higher than background values of ~0.05 pcm^3/g through the mid-Tortonian up to meter level 119.5. All this suggests that the Rossini Member records the tail of the Veritas interplanetary dust particle cascade, but the general SST cooling and the large temperature excursions recorded in this interval were probably related to local environmental changes caused by intense regional volcanism rather than a global climate change forced by orbital cycles or by the effects of a petering-out extraterrestrial event. What is more relevant for the understanding of the Veritas event is the subtle SST negative shift recorded by Tzanova et al. (2015) at meter level 119.5, exactly at the inception of the main ^{3}He

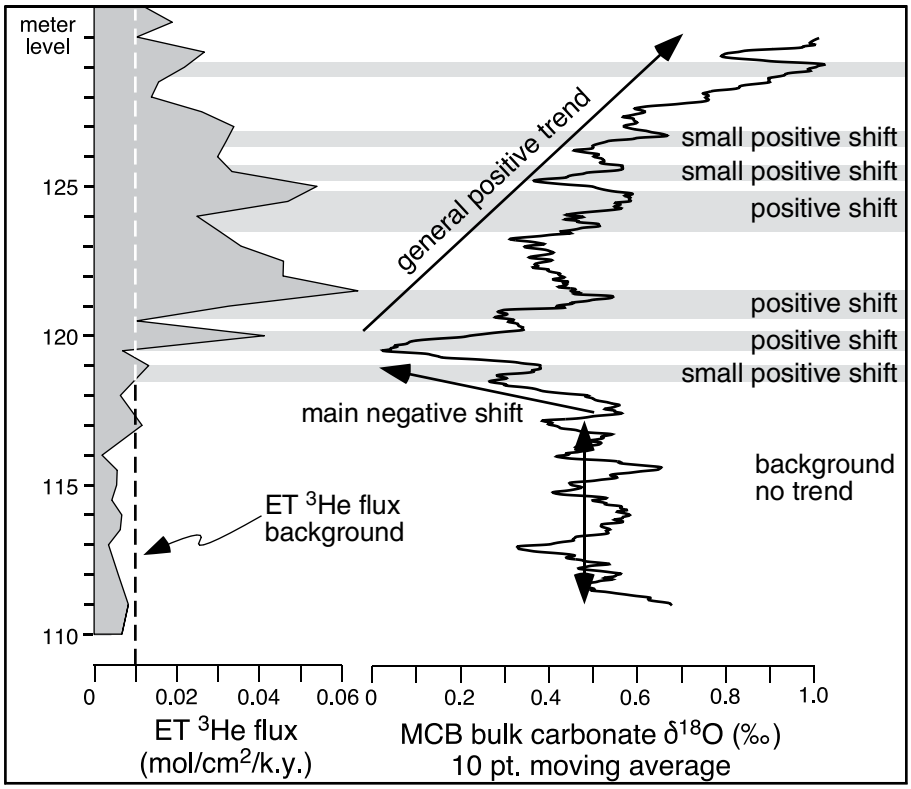

Figure 13. Correlation between the variations of the extraterrestrial (ET) ^{3}He flux and the excursions of the δ^{18}O record through the Monte dei Corvi Beach (MCB) section.

Downloaded from https://pubs.geoscienceworld.org/gsa/gsabulletin/article-pdf/129/9-10/1357/2615686/1357.pdf
by University of Western Ontario user

anomaly (see Fig. 2). All through the enhanced ^{3}He interval, the SST decreases monotonically from ~27.5 °C to ~26.0 °C. This slight decay of the SST reflects the general positive trend in the δ^{18}O through this interval, which, nevertheless, is punctuated by six minor positive shifts corresponding to the peaks of ^{3}He concentration (Fig. 13). Therefore, there seems to be a coherent relationship among the local SST changes, the global climate changes, and the Veritas event. The conundrum here is that the mean δ^{18}O values through the enhanced ^{3}He interval are lower than those of the preceding Tortonian values. The change is sharp and denoted by a prominent negative shift at ~117.5 m (ca. 8.65 Ma), which is readily recognizable in the oceanic δ^{18}O record of Zachos et al. (2001), and the continental δD record of Huang et al. (2007). This indicates that during the Veritas interplanetary dust particle cascade, global climatic conditions were actually warmer and wetter than in the preceding Tortonian interval, but the alkenone record indicates that local SSTs were instead slightly lower. A possible explanation of this apparent paradox may be that the cascade of asteroidal debris, which after the Veritas breakup came in pulses, caused repeated climate changes toward cooler temperatures when particulate matter derived from a myriad of small meteoritic impacts diminished insolation by rendering the atmosphere more opaque (cf. e.g., Muller, 2001; Pavlov et al., 2005), and then switching to warm spells in the following period with an atmosphere still polluted by greenhouse gases. Globally, the first warm spell would have affected the glacioeustatic system, which responded with an enrichment of ^{16}O in seawater (negative δ^{18}O shift), and a global sea-level rise, but locally, the impact-induced cold spells may have prevailed, leading to a slight decrease of the SST.

CONCLUSIONS

Our chemostratigraphic analysis of the Upper Tortonian Monte dei Corvi section shows an extraterrestrial ^{3}He anomaly produced by fivefold increase in interplanetary dust particle influx. This probably originated from a collisional event in the asteroid belt that created the Veritas family of asteroids. Cyclostratigraphic spectral analysis of a high-resolution MS proxy series yielded a spectrum of significant frequency peaks compatible with Milankovitch cycles (i.e., precession, tilt, and eccentricity), which promoted an eccentricity-based tuning of the section using the orbital solution of Laskar et al. (2004). From this, we derived an astrochronological age of 8.47 ± 0.05 Ma for the inception of the extraterrestrial ^{3}He influx, and an age of 8.69 ± 0.05 Ma for the actual asteroidal breakup, which is consistent with, yet more precise than, the age of 8.3 ± 0.5 Ma calculated by astrophysical means by Nesvorny et al., (2003) for the Veritas breakup. The ^{3}He influx came in four main pulses before drastically dropping down at ca. 7.7 Ma and then petering out to background levels at ca. 6.9 Ma. Spectral analysis and cross-correlation of other four environmental proxies (i.e., biogenic calcium carbonate and organic carbon contents, and oxygen and carbon isotopes), as well as existing high-resolution SST data from the same section, suggest that global and local environmental conditions were altered, and orbitally forced climatic cycles were obscured by the interference of random forces. This leads us to the hypothesis that pulses of extraterrestrial material produced by the Veritas breakup cascading on Earth caused periodic opacification of the atmosphere, with consequent alteration of global and local environmental conditions. In summary, chemostratigraphic evidence of a collisional event that created the Veritas family of asteroids and coincident climate perturbations on Earth suggest yet another form of interaction between Earth and the solar system, which, nevertheless, may help in fixing boundaries for future modeling of asteroidal breakups, and their possible effects on Earth's environmental and climatic systems.

ACKNOWLEDGMENTS

This research was supported by the Research Foundation Flanders (FWO grants G0B8513N and G009113N), the Hercules Foundation for the upgrade of the Vrije Universiteit Brussel Stable Isotope Laboratory (Philippe Claeys), and support from the Flemish Agency for Innovation by Science and Technology (IWT; to Niels De Winter). We thank the Association "Le Montagne di San Francesco" of Coldigioco for logistical support while working on this research project. We would also like to thank Beatrice Cecchin for helping to collect the samples in the Monte dei Corvi Beach section in 2009, and preparing them for laboratory analyses at the University of Vienna. A special thanks goes to Timothy Herbert and Alexandrina Tzanova (Brown University, Rhode Island) for providing the sea-surface temperature data of the Monte dei Corvi Beach section, Laura Cleaveland-Peterson (Luther College, Iowa) for providing the raw magnetic susceptibility data from the Monte dei Corvi section, Mario Sprovieri (L'Istituto per l'Ambiente Marino Costiero del Consiglio Nazionale delle Ricerche [CNR-IAMC], Italy) for providing the raw oxygen and carbon stable isotope data from the Cenomanian–Turonian section of Bottaccione, and Heather Stoll (University of Oviedo, Spain) for providing the raw oxygen and carbon stable isotope data from the Cenomanian–Turonian section of Contessa. We would like to thank David Bice, Jan Smit, Maurizio Mainiero, and Rodolfo Coccioni for sharing their knowledge and discussions about the stratigraphic succession at Monte dei Corvi. Last, but not least, we would like to thank David Bice, Birger Schmitz, and two other undisclosed *GSA Bulletin* reviewers, as well as Editors H. Dypvik and A. Cavosie, for their useful and constructive comments and suggestions, which greatly helped us to improve the form and contents of this paper.

REFERENCES CITED

Alvarez, W., Cocozza, T., and Wezel, F.C., 1974, Fragmentation of the Alpine orogenic belt by microplate dispersal: Nature, v. 248, p. 309–314, doi:10.1038/248309a0.

Alvarez, W., Colacicchi, R., and Montanari, A., 1985, Synsedimentary slides and bedding formation in Apennines pelagic limestones: Journal of Sedimentary Petrology, v. 55, p. 720–734.

Argnani, A., Fontana, D., Stefani, C., and Zuffa, G.G., 2006, Palaeogeography of the Upper Cretaceous–Eocene carbonate turbidites of the Northern Apennines from provenance studies, *in* Moratti, G., and Chalouan, A., eds., Tectonics of the Western Mediterranean and North Africa: Geological Society, London, Special Publication 262, p. 259–275, doi:10.1144/GSL.SP.2006.262.01.16.

Beaudoin, B., M'Ban, E.P., Montanari, A., and Pinault, M., 1996, Stratigraphie haute resolution (<20 ka) dans le Cenomanien du bassin de Marches-Ombrie (Italie): Comptes Rendus de l'Académie de Sciences, v. 323, p. 689–696.

Bice, D., Montanari, A., Vučetić, V., and Vučetić, M., 2011, The influence of regional and global climatic oscillations on Croatian climate: International Journal of Climatology (Wiley online: The Library), v. 32, no. 10, p. 1537–1557, doi:10.1002/joc.2372.

Brown, P.G., and 27 others, 2013, A 500-kiloton airburst over Chelyabinsk and an enhanced hazard from small impactors: Nature, v. 503, p. 238–241.

Brown, R., Cleaveland, L., Bice, D.M., Koeberl, C., and Montanari, A., 2009, Cyclostratigraphic analysis and astronomical tuning of the Eocene-Oligocene boundary GSSP at Massignano (Italy), *in* Koeberl, C., and Montanari, A., eds., The Late Eocene Earth: Geological Society of America Special Paper 452, p. 119–138, doi:10.1130/2009.2452(08).

Castellarin, A., Colacicchi, R., Praturlon, A., and Cantelli, C., 1982, The Jurassic–Lower Pliocene history of the Anzio-Ancona Line (central Italy): Memorie della Società Geologica Italiana, v. 24, p. 325–336.

Channell, J.E.T., D'Argenio, B., and Horvath, F., 1979, Adria, the African promontory in Mesozoic Mediterranean palaeogeography: Earth-Science Reviews, v. 15, p. 213–292, doi:10.1016/0012-8252(79)90083-7.

Cleaveland, L.C., 2001, Calcium Carbonate and Magnetic Susceptibility Analysis at Monte dei Corvi, Italy: Trends in the Mediterranean Climate Proxy Record during Middle Miocene Ice Sheet Expansion [Senior thesis]: Northfield, Minnesota, Carleton College, 34 p.

Cleaveland, L.C., Jensen, J., Goese, S., Bice, D.M., and Montanari, A., 2002, Cyclostratigraphic analysis of pelagic carbonates at Monte dei Corvi (Ancona, Italy) and astronomical correlation of the Serravallian-Tortonian boundary: Geology, v. 30, p. 931–934, doi:10.1130/0091-7613(2002)030<0931:CAOPCA>2.0.CO;2.

Coccioni, R., Moretti, E., Nesci, O., Savelli, D., Tramontana, M., Veneri, F., and Astracedi, M., 1993, Carta Geologica con Itinerari Escursionistici: Firenze, Italy, Parco Regionale del Conero, S.E.L.C.A., scale 1:20,000.

Cornamusini, G., Lazzarotto, A., Merlini, S., and Pascucci, V., 2002, Eocene-Miocene evolution of the north Tyrrhenian Sea: Bollettino della Società Geologica Italiana, v. 1, p. 769–787.

D'Argenio, B., 1970, Evoluzione geottettonica comparata tra alcune piattaforme carbonatiche dei Mediterranei Europeo ed Americano: Atti Accademia Pontiana, v. 20, p. 3–34.

Farinella, P., Foschini, L., Froeschlé, Ch., Gonczi, R., Jopek, T.J., Longo, G., and Michel, P., 2001, Probable asteroidal origin of the Tunguska cosmic body: Astronomy and Astrophysics, v. 377, p. 1081–1097, doi:10.1051/0004-6361:20011054.

Farley, K.A., Montanari, A., Shoemaker, E., and Shoemaker, C., 1998, Geochemical evidence for a comet shower in the late Eocene: Science, v. 280, p. 1250–1253, doi:10.1126/science.280.5367.1250.

Farley, K.A., Vokrouhlicky, D., Bottke, W.F., and Nesvorny, D., 2006, A late Miocene dust shower from the breakup of an asteroid in the main belt: Nature, v. 439, p. 295–297, doi:10.1038/nature04391.

Farley, K., Montanari, A., and Coccioni, R., 2012, A record of the extraterrestrial ^{3}He flux through the Late Cretaceous: Geochimica et Cosmochimica Acta, v. 84, p. 314–328.

Downloaded from https://pubs.geoscienceworld.org/gsa/gsabulletin/article-pdf/129/9-10/1357/2615686/1357.pdf
by University of Western Ontario user

Ferriére, L., and Robin, E., 2009, Composition and origin of Ni-rich spinel from Cretaceous-Tertiary boundary: Lunar and Planetary Science Conference Abstracts, v. XL, paper 1812.

Galeotti, S., von der Heydt, A., Huber, M., Bice, D., Dijkstra, H., Jilbert, T., Lanci, L., and Reichart, G.-J., 2010, Evidence for active El Niño–Southern Oscillation variability in the late Miocene greenhouse climate: Geology, v. 38, p. 418–422, doi:10.1130/G30629.1.

Haq, B.U., Hardenbol, J., and Vail, P.R., 1987, Chronology of fluctuating sea levels since the Triassic: Science, v. 235, p. 1156–1167, doi:10.1126/science.235.4793.1156.

Hilgen, F., Abdul Aziz, H., Krijgsman, W., Raffi, I., and Turco, E., 2003, Integrated stratigraphy and astrochronology of the Serravallian and Lower Tortonian at Monte dei Corvi (Middle–Upper Miocene, northern Italy): Palaeogeography, Palaeoclimatology, Palaeoecology, v. 199, p. 229–264, doi:10.1016/S0031-0182(03)00505-4.

Hilgen, F., Iaccarino, S., Krijgsman, W., Montanari, A., Raffi, I., Turco, E., and Zachariasse, W.-J., 2005, The global boundary stratotype section and point (GSSP) of the Tortonian Stage (Upper Miocene) at Monte dei Corvi: Episodes, v. 28, p. 1–12.

Hsü, K.J., Cita, M.B., and Ryan, W.B.F., 1973, The origin of the Mediterranean evaporites, *in* Initial Report of the Deep Sea Drilling Project, Leg 13: Washington, D.C., U.S. Government Printing Office, p. 1203–1231.

Hsü, K.J., Montadert, L., Bernoulli, D., Cita, M.B., Erickson, A., Garrison, R.E., Kidd, R.B., Milihres, X., Miller, C., and Wright, R., 1978, History of the Mediterranean salinity crisis: Initial Report Deep Sea Drilling Project, Volume 42A: Washington, D.C., U.S. Government Printing Office, p. 1053–1078.

Huang, Y., Clemens, S.C., Liu, W., and Prell, W.L., 2007, Large-scale hydrological change drove the late Miocene C4 plant expansion in the Himalayan foreland and Arabian Peninsula: Geology, v. 35, p. 531–534, doi:10.1130/G23666A.1.

Huber, M., McDonald, I., and Koeberl, C., 2014, Petrography and geochemistry of ejecta from the Sudbury impact event: Meteoritics & Planetary Science, v. 49, p. 1749–1768, doi:10.1111/maps.12352.

Hüsing, S.K., Hilgen, F.J., Aziz, H.A., and Krijgsman, W., 2007, Completing the Neogene geological time scale between 8.5 and 12.5 Ma: Earth and Planetary Science Letters, v. 253, p. 340–358, doi:10.1016/j.epsl.2006.10.036.

Hüsing, S.K., Kuiper, K.F., Link, W., Hilgen, F.J., and Krijgsman, W., 2009, The Upper Tortonian–Lower Messinian at Monte dei Corvi (Northern Apennines, Italy): Completing a Mediterranean reference section for the Tortonian Stage: Earth and Planetary Science Letters, v. 282, p. 140–157, doi:10.1016/j.epsl.2009.03.010.

Hüsing, S.K., Cascella, A., Hilgen, F.J., Krijgsman, W., Kuiper, K.F., Turco, E., and Wilson, D., 2010, Astrochronology of the Mediterranean Langhian between 15.29 and 14.17 Ma: Earth and Planetary Science Letters, v. 290, p. 254–269.

Knežević, Z., Tsiganis, K., and Varvoglis, K., 2006, Age of the Veritas asteroid family from two independent estimates: Publications of the Astronomical Observatory of Belgrade, v. 80, p. 161–166.

Koeberl, C., 2009, Late Eocene impact craters and impactoclastic layers—An overview, *in* Koeberl, C., and Montanari, A., eds., The Late Eocene Earth: Geological Society of America Special Paper 452, p. 119–138, doi:10.1130/2009.2452(08).

Koeberl, C., 2014, The geochemistry and cosmochemistry of impacts, *in* Holland, H.D., and Turekian, K.K., eds., Treatise on Geochemistry, Volume 2. Planets, Asteroids, Comets and the Solar System (2nd ed.): Oxford, UK, Elsevier, p. 73–118.

Krijgsman, W., Hilgen, F.J., Raffi, I., Sierro, F.J., and Wilson, D., 1999, Chronology, causes, and progression of the Messinian salinity crisis: Nature, v. 400, p. 652–655, doi:10.1038/23231.

Laskar, J., Robutel, P., Joutel, F., Gastineau, M., Correia, A.C.M., and Levrard, B., 2004, A long-term numerical solution for the insolation quantities of the Earth: Astronomy and Astrophysics, v. 428, p. 261–285, doi:10.1051/0004-6361:20041335.

Laurenzi, M., Tateo, F., Villa, I.M., and Vai, G.B., 1997, New radiometric datings bracketing the Tortonian/Messinian boundary in the Romagna potential stratotype sections (northern Italy), *in* Montanari, A., Odin, G.S., and Coccioni, R., eds., Miocene Integrated Stratigraphy: Amsterdam, Netherlands, Elsevier, p. 493–521.

Mader, D., and Koeberl, C., 2009, Using instrumental neutron activation analysis for geochemical analyses of terrestrial impact structures: Current analytical procedures at the University of Vienna gamma spectrometry laboratory: Applied Radiation and Isotopes, v. 67, p. 2100–2103, doi:10.1016/j.apradiso.2009.04.014.

Mader, D., Cleaveland, L., Koeberl, C., Bice, D., and Montanari, A., 2004, High-resolution geochemical proxies of a short Langhian pelagic sequence at the Cònero Riviera, Ancona (Italy): Some palaeoenvironmental and cyclostratigraphic considerations: Palaeogeography, Palaeoclimatology, Palaeoecology, v. 211, p. 325–344, doi:10.1016/j.palaeo.2004.06.001.

Marroni, M., Molli, G., Ottria, G., and Pandolfi, L., 2001, Tectono-sedimentary evolution of the External Liguride units (Northern Apennines, Italy): Insights in the pre-collisional history of a fossil ocean-continent transition zone: Geodinamica Acta, v. 14, p. 307–320, doi:10.1080/09853111.2001.11432449.

M'Ban, E.P., 1996, Evolution de la Sedimentation Pelagique au Cretace Superieur des Marches et de l'Ombre (Italie Centrale): Litho.-Biostratigraphie, Géochemie, Paléoenvironnment [Doctorate thesis]: Memoir de Sciences de la Terre, University of Paris 6, 247 p.

Menichetti, M., Coccioni, R., and Montanari, A., eds., 2016, The Stratigraphic Record of Gubbio: Integrated Stratigraphy of the Late Cretaceous–Paleogene Umbria-Marche Pelagic Basin: Geological Society of America Special Paper 524, 175 p., doi:10.1130/9780813725246.

Michel, P., Jutzi, M., Richardson, D.C., and Benz, W., 2010, The Asteroid Veritas: An intruder in a family named after it?: Icarus, v. 211, p. 535–545, doi:10.1016/j.icarus.2010.10.012.

Montanari, A., and Koeberl, C., 2000, Impact Stratigraphy: The Italian Record: Lecture Notes in Earth Sciences: Berlin, Springer, 364 p.

Montanari, A., Asaro, F., Kennett, J.P., and Michel, E., 1993, Iridium anomalies of late Eocene age at Massignano (Italy), and in ODP Site 689B (Maud Rise, Antarctica): Palaios, v. 8, p. 420–437, doi:10.2307/3515017.

Montanari, A., Beaudoin, B., Chan, L., Coccioni, R., Deino, A., DePaolo, D.J., Emmanuel, L., Fornaciari, E.S., Kruge, M., Lundblad, S., Mozzato, C., Portier, E., Renard, M., Rio, D., Sandroni, P., and Stankiewicz, A., 1997, Integrated stratigraphy of the Middle to Upper Miocene pelagic sequence of the Cònero Riviera (Ancona, Italy), *in* Montanari, A., Odin, G.S., and Coccioni, R., eds., Miocene Stratigraphy: An Integrated Approach: Amsterdam, Elsevier Science B.V., Developments in Paleontology and Stratigraphy 15, p. 409–450.

Montanari, A., Campo Bagatin, A., and Farinella, P., 1998, Earth cratering record and impact energy flux in the last 150 Ma: Planetary and Space Science, v. 46, p. 271–281, doi:10.1016/S0032-0633(97)00130-X.

Mukhopadhyay, S., Farley, K.A., and Montanari, A., 2001, A 35 Myr record of helium in pelagic limestones: Implications for interplanetary dust accretion in the early Maastrichtian to the middle Eocene: Geochimica et Cosmochimica Acta, v. 65, p. 653–669, doi:10.1016/S0016-7037(00)00555-X.

Muller, R.A., 2001, Glacial cycles and interplanetary dust, *in* Peucker-Ehrenbrink, B., and Schmitz, B., eds., Accretion of Extraterrestrial Matter Throughout Earth's History: Dordrecht, Netherlands, Kluwer, p. 143–161, doi:10.1007/978-1-4419-8694-8_9.

Muller, R.A., and MacDonald, G.J., 2000, Ice Ages and Astronomical Causes: Data, Spectral Analysis and Mechanisms: Chichester, UK, Praxis Publishing Ltd., 318 p.

Nesvorny, D., Bottke, W.F., Levison, H.F., and Dones, L., 2003, Recent origin of the solar system dust bands: The Astrophysical Journal, v. 591, p. 486–497, doi:10.1086/374807.

Odin, G.S., Vai, G.B., Cosca, M., Tateo, F., and Hunziker, J.C., 1997a, Contribution to the Tortonian/Messinian boundary in the Faenza area (Romagna, Italy), *in* Montanari, A., Odin, G.S., and Coccioni, R., eds., Miocene Stratigraphy: An Integrated Approach: Amsterdam, Elsevier Science B.V., Developments in Paleontology and Stratigraphy 15, p. 521–530.

Odin, G.S., Montanari, A., and Coccioni, R., 1997b, Chronostratigraphy of Miocene stages: A proposal for the definition of precise boundaries, *in* Montanari, A., Odin, G.S., and Coccioni, R., eds., Miocene Stratigraphy: An Integrated Approach: Amsterdam, Elsevier Science B.V., Developments in Paleontology and Stratigraphy 15, p. 596–629.

Pavlov, A.A., Toon, O.B., Pavlov, A.K., Bally, J., and Pollard, D., 2005, Passing through a giant molecular cloud: Snowball glaciations produced by interstellar dust: Geophysical Research Letters, v. 32, L03705, doi:10.1029/2004GL021890.

Povinec, P.P., Laubenstein, M., Jull, A.J.T., Ferrière, L., Brandstätter, F., Sýkora, I., Masarik, J., Beno, J., Kovácik, A., Topa, D., and Koeberl, C., 2015, Cosmogenic radionuclides and mineralogical properties of the Chelyabinsk (LL5) meteorite: What do we learn about the meteoroid?: Meteoritics & Planetary Science, v. 50, p. 273–286, doi:10.1111/maps.12419.

Schmitz, B., Boschi, S., Cronholm, A., Heck, P.R., Monechi, S., Montanari, A., and Terfelt, F., 2015, Fragments of late Eocene Earth-impacting asteroids linked to disturbance of asteroid belt: Earth and Planetary Science Letters, v. 425, p. 77–83, doi:10.1016/j.epsl.2015.05.041.

Sprovieri, M., Samatino, N., Pelosi, N., Batenburg, S.J., Coccioni, R., Iavarone, M., and Mazzola, S., 2013, Late Cretaceous orbitally-paced carbon isotope stratigraphy from the Bottaccione Gorge (Italy): Palaeogeography, Palaeoclimatology, Palaeoecology, v. 379, p. 81–94, doi:10.1016/j.palaeo.2013.04.006.

Stoll, H.M., and Schrag, D.P., 2000, High-resolution stable isotope records from the Upper Cretaceous rocks of Italy and Spain: Glacial episodes in a greenhouse planet?: Geological Society of America Bulletin, v. 112, p. 308–319, doi:10.1130/0016-7606(2000)112<308:HSIRFT>2.0.CO;2.

Tagle, R., and Claeys, P., 2004, Comet or asteroid shower in the late Eocene?: Science, v. 305, p. 492, doi:10.1126/science.1098481.

Treves, B., 1984, Orogenic belts as accretionary prisms: The example of the Northern Apennines: Ofioliti, v. 9, p. 577–618.

Tzanova, A., Herbert, T.D., and Peterson, L., 2015, Cooling Mediterranean Sea surface temperatures during the late Miocene provide a climate context for evolutionary transitions in Africa and Eurasia: Earth and Planetary Science Letters, v. 419, p. 71–80, doi:10.1016/j.epsl.2015.03.016.

Vai, G.B., 1997, Cyclostratigraphic estimate of the Messinian Stage duration, *in* Montanari, A., Odin, G.S., and Coccioni, R., eds., Miocene Stratigraphy: An Integrated Approach: Amsterdam, Elsevier Science B.V., Developments in Paleontology and Stratigraphy 15, p. 463–476.

Wendler, I., 2013, A critical evaluation of carbon isotope stratigraphy and biostratigraphic implications for Late Cretaceous global correlation: Earth-Science Reviews, v. 126, p. 116–146, doi:10.1016/j.earscirev.2013.08.003.

Wotzlaw, J.F., Hüsing, S.K., Hilgen, F.J., and Schaltegger, U., 2014, High-precision U-Pb geochronology of astronomically dated ash beds from the Mediterranean Miocene: Earth and Planetary Science Letters, v. 407, p. 19–34, doi:10.1016/j.epsl.2014.09.025.

Zachos, J.C., Pagani, M., Sloan, L., Thomas, E., and Billups, K., 2001, Trends, rhythms, and aberrations in global climate 65 Ma to present: Science, v. 292, p. 686–692, doi:10.1126/science.1059412.

Science Editor: Aaron J. Cavosie
Associate Editor: Henning Dypvik

Manuscript Received 21 December 2015
Revised Manuscript Received 24 January 2017
Manuscript Accepted April 19 2017

Printed in the USA

Downloaded from https://pubs.geoscienceworld.org/gsa/gsabulletin/article-pdf/129/9-10/1357/2615686/1357.pdf
by University of Western Ontario user